Glucose and sucrose signaling modules regulate the arabidopsis juvenile-to-adult phase transition

Cell Reports

Article

Glucose- and sucrose-signaling modules regulate the *Arabidopsis* juvenile-to-adult phase transition

Graphical abstract

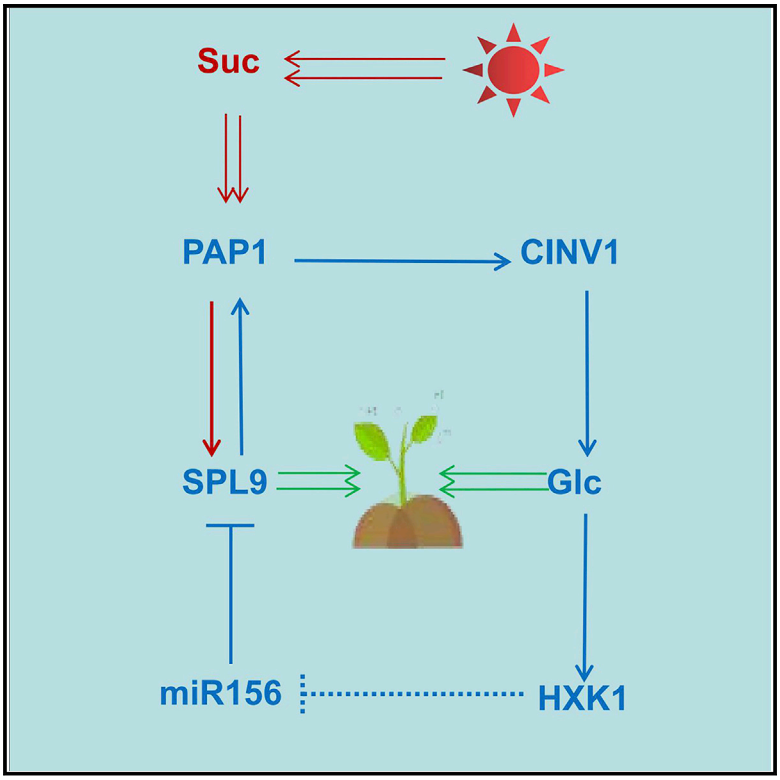

Highlights

- CINV1/2 are key endogenous factors that control the *Arabidopsis* juvenile-to-adult transition
- A glucose-signaling feed-forward loop dynamically controls the juvenile-to-adult transition
- A sucrose-signaling pathway regulates the juvenile-to-adult transition

Authors

Lai-Sheng Meng, Qin-Xin Bao, Xin-Rong Mu, ..., Chang-Yue Liu, Yue Fei, Gary J. Loake

Correspondence

menglsh@jsnu.edu.cn (L.-S.M.), gloake@ed.ac.uk (G.J.L.)

In brief

Meng et al. identify a glucose-signaling feed-forward loop and a sucrose-signaling pathway that synergistically regulate the *Arabidopsis* juvenile-to-adult transition. This glucose feed-forward loop controls CINV1 activity to convert sucrose into glucose signaling to dynamically control juvenile-to-adult transition.

Meng et al., 2021, Cell Reports *36*, 109348
July 13, 2021
https://doi.org/10.1016/j.celrep.2021.109348

CellPress

Cell Reports

CellPress
OPEN ACCESS

Article

Glucose- and sucrose-signaling modules regulate the *Arabidopsis* juvenile-to-adult phase transition

Lai-Sheng Meng,[1,4,5,*] Qin-Xin Bao,[1,4] Xin-Rong Mu,[1,4] Chen Tong,[1,4] Xiao-Ying Cao,[1] Jin-Jin Huang,[1] Li-Na Xue,[1] Chang-Yue Liu,[1] Yue Fei,[1] and Gary J. Loake[2,3,*]

[1]The Key Laboratory of Biotechnology for Medicinal Plants of Jiangsu Province, School of Life Science, Jiangsu Normal University, Xuzhou, Jiangsu 221116, People's Republic of China

[2]Jiangsu Normal University–Edinburgh University, Centre for Transformative Biotechnology of Medicinal and Food Plants, Jiangsu Normal University, 101 Shanghai Road, Xuzhou, People's Republic of China

[3]Institute of Molecular Plant Sciences, School of Biological Sciences, Edinburgh University, King's Buildings, Mayfield Road, Edinburgh EH9 3JR, UK

[4]These authors contributed equally

[5]Lead contact

*Correspondence: menglsh@jsnu.edu.cn (L.-S.M.), gloake@ed.ac.uk (G.J.L.)

https://doi.org/10.1016/j.celrep.2021.109348

SUMMARY

CINV1, converting sucrose into glucose and fructose, is a key entry of carbon into cellular metabolism, and HXK1 functions as a pivotal sensor for glucose. Exogenous sugars trigger the *Arabidopsis* juvenile-to-adult phase transition via a miR156A/SPL module. However, the endogenous factors that regulate this process remain unclear. In this study, we show that sucrose specifically induced the PAP1 transcription factor directly and positively controls CINV1 activity. Furthermore, we identify a glucose feed-forward loop (sucrose-CINV1-glucose-HXK1-miR156-SPL9-PAP1-CINV1-glucose) that controls CINV1 activity to convert sucrose into glucose signaling to dynamically control the juvenile-to-adult phase transition. Moreover, PAP1 directly binds to the *SPL9* promoter, activating *SPL9* expression and triggering the sucrose-signaling-mediated juvenile-to-adult phase transition. Therefore, a glucose-signaling feed-forward loop and a sucrose-signaling pathway synergistically regulate the *Arabidopsis* juvenile-to-adult phase transition. Collectively, we identify a molecular link between the major photosynthate sucrose, the entry point of carbon into cellular metabolism, and the plant juvenile-to-adult phase transition.

INTRODUCTION

Vegetative phase change is the transition from the juvenile to adult vegetative phase. During the juvenile phase, plants are not able to initiate reproductive development leading to flowering, and they are also insensitive to numerous environmental signals, including vernalization and photoperiod (Matsoukas et al., 2013; Sgamma et al., 2014; Matsoukas., 2014; Guo et al., 2017). In *Arabidopsis*, vegetative phase change is characterized through an enhancement in the leaf length/width ratio, alternations in the production of trichomes on the abaxial side of the leaf blade, a decline in cell size, and an enhancement in the degree of serration of the leaf margin (Usami et al., 2009).

miR156 is a central factor in the regulation of the juvenile-to-adult transition, and an increase of sugar promotes *miR156* downregulation to trigger the juvenile-to-adult transition (Yu et al., 2013; Yang et al., 2013). Whereas the expression of miR156 decreases over time during vegetative phase change, the expression of its targets, squamosa promoter binding protein-like (SPL) transcriptional factors, for example, SPL3/4/5/9, are enhanced during this process (Wu et al., 2009; Yu et al., 2013; Yang et al., 2013). This juvenile-to-adult phase transition is thought to occur following an increase in glucose or a related metabolite (such as trehalose) beyond a threshold level. Whereas exogenous sucrose/glucose triggers the juvenile-to-adult phase transition by a miR156A/SPL9 cascade, the endogenous factors that regulate this process remain unclear.

Increasing exogenous sugar results in the suppression of miR156/157 abundance via transcriptional and post-transcriptional mechanisms, and this binary control strategy is thought to convey robust repression of miR156, leading to the juvenile-to-adult transition in plants (Yu et al., 2013; Yang et al., 2013; He et al., 2018). This is thought to lead to a concomitant enhancement in transcript abundance of the miR156 target genes encoding SPL3/4/5/9 transcription factors and miR172 (Wu et al., 2009; Wang et al., 2009; Kim et al., 2012; Jung et al., 2011, 2012; Yu et al., 2013). The enhancement in SPLs at the shoot apical meristem (SAM) results in the transcription of floral meristem initiation genes (Schwab et al., 2005; Schwarz et al., 2008; Wang et al., 2009; Yamaguchi et al., 2009), and the increase in SPL9 at leaf blades promotes the juvenile-to-adult phase transition and flowering by activation of MADS-box and miR172 genes (Wang et al., 2009; Jung et al., 2011). In parallel, the expression of miR172 is thought to activate *FLOWERING*

LOCUS T (*FT*) transcription in leaf blades by suppression of the *AP2*-like transcripts encoded by *SCHNARCHZAPFEN* (*SNZ*), *SCHLAFMÜTZE* (*SMZ*), and *TARGET OF EAT 1–3* (*TOE1–3*) (Mathieu et al., 2009; Jung et al., 2011). In addition to modulation by sugars, *miR156* expression is also controlled through other exogenous cues, including phosphate starvation (Hsieh et al., 2009), temperature (Lee et al., 2010; Xin et al., 2010; Yu et al., 2012), and CO_2 concentration (May et al., 2013).

The ability of sugars to function as key signal molecules across biological kingdoms has been well documented (Rolland et al., 2001). Sugars are thought to regulate both plant juvenile-to-adult and adult-to-reproductive phase transitions through their function as key signaling molecules and energy sources. Most plant cells acquire their essential carbon from sucrose; however, this sugar is not utilized directly. Cytosolic invertase (CINV) irreversibly catalyzes the conversion of sucrose to glucose and fructose, whereas sucrose synthase (SUS) reversibly catalyzes the conversion of sucrose to fructose and UDP glucose (Lou et al., 2007). Significantly, the gateway of carbon from sucrose into cellular metabolism appears to be controlled principally by CINV1/2 (two of the nine CINV isoforms) rather than by SUS, which is not essential for normal plant growth and development (Barratt et al., 2009). An additional INV, vacuolar INV (VINV), regulates plant growth by its impact on vacuolar osmotic potential (Sergeeva et al., 2006; Barratt et al., 2009), rather than through cellular signaling. As sugars trigger the *Arabidopsis* juvenile-to-adult phase transition through a signal function (Yang et al., 2013), VINV may not be involved in this process. In contrast, CINV1/2 activity provides a key point of control for coordinating sucrose catabolism with sugar signaling/metabolism-mediated plant growth and development. However, this enzyme has not been previously linked to phase transitions.

PAP1 (production of anthocyanin pigment 1), a putative MYB domain-containing transcription factor (MYB75), is considered a key integration point for a variety of internal and external stimuli that influence the biosynthesis of anthocyanins (Teng et al., 2005; Das et al., 2012; Jaakola, 2013). Significantly, sucrose, but not other sugars, can specifically induce *PAP1* expression (Teng et al., 2005; Solfanelli et al., 2006).

In this study, we show that a glucose feed-forward loop dynamically converts sucrose signaling into glucose signaling in leaves to trigger the plant juvenile-to-adult phase transition. In addition, the major photosynthate, sucrose, specifically induces *PAP1* expression and this transcription factor in turn directly and positively regulates *SPL9* expression to promote the plant juvenile-to-adult phase transition.

RESULTS

PAP1 positively regulates the juvenile-to-adult transition

A miR156-targeted SPL transcription factor, SPL9, regulates the *Arabidopsis* juvenile-to-adult transition mediated by sugar signaling (Yu et al., 2013; Yang et al., 2013), and SPL9 may directly interact with PAP1 (Gou et al., 2011). Sucrose, but not other sugars, specifically promotes mRNA accumulation of *PAP1* (Teng et al., 2005; Solfanelli et al., 2006). Collectively, these findings suggest that PAP1 may be linked to regulation of the juvenile-to-adult transition.

To address this hypothesis, we utilized three kinds of *Arabidopsis PAP1*-expressing transgenes to analyze potential PAP1 function in phase transition: (1) cauliflower mosaic virus *35S* (*35S*):*PAP1*, (2) an *ASYMMETRIC LEAVES 1* (*AS1*) promoter, specifically expressed in the leaf and meristem (Guo et al., 2008), driving expression of a *PAP1-green fluorescent protein* (*GFP*) fusion; and, (3) *PAP1* expressed via an activation tag-generated dominant mutant allele of this transcription factor, *pap1-dominant* (*pap1-D*) (Qi et al., 2011) (Figure S1).

Under short days (10-h light/14-h dark cycle) and standard light conditions (130 μmol quanta PAR m^{-2} s^{-1}), 18-day-old *35S:PAP1*, *AS1pro:PAP1-GFP*, and *pap1-D* seedlings all showed a shortened juvenile phase (Figure 1A). That is, the ratio of leaf blade length to width, the first leaf with abaxial trichomes, and *miR156A* expression were more closely related to those of adult leaves in these *PAP1* overexpressing plants relative to the wild-type (Figures 1C, 1E, and 1F). However, under the same conditions, plants of a *PAP1* loss-of-function mutant, *myb75-1*, exhibited no obvious prolonged juvenile phase. It has been reported that "super short" days (8-h light/16-h dark cycle) and "low light" (80 μmol quanta PAR m^{-2} s^{-1}) can significantly elongate the plant life cycle and be used to distinguishing between a possible developmental phenotype (Yang et al., 2013). Under super short days and low light conditions, *myb75-1* plants exhibited a prolonged juvenile phase (Figure 1B). Thus, the ratio of leaf blade length to width, the first leaf with abaxial trichomes, and *miR156A* expression more closely resembled those of juvenile plants (Figures 1D–1F). Furthermore, an increase of glucose levels in *PAP1* overexpressing plants (Figure 1G) correlated with a shortened juvenile phase. As INV function is a key generator of glucose, the increase of this hexose may be due to the enhancement of INV activity. Indeed, INV activity was enhanced in *PAP1* overexpressing plants (Figure 1H). In contrast, there was a decrease in glucose levels in *myb75-1* plants (Figure 1G), which exhibited a delayed juvenile-to-adult transition. Furthermore, *myb75-1* plants showed a decrease of INV activity (Figure 1H).

To confirm PAP1 function in phase transition, we utilized two different *Arabidopsis* accessions, Cvi and C24. PAP1 has been identified as a sucrose-activated transcription factor in a previous analysis of sucrose-induced anthocyanin accumulation in 43 *Arabidopsis* accessions (Teng et al., 2005). The activity of PAP1 in Cvi and C24 accessions was impaired as a result of natural variation in the PAP1 amino acid sequence. Similar to *myb75-1* plants, Cvi and C24 seedlings presented a prolonged juvenile phase (Figure S2).

Taken together, these data indicate that PAP1 positively regulates the *Arabidopsis* juvenile-to-adult transition.

PAP1 promotes *CINV1/2* expression and elevates CINV1/2 activity by glucose signaling or by converting sucrose signaling into glucose signaling

The MYB transcription factor PAP1/MYB75 is specifically induced by sucrose signaling to stimulate anthocyanin biosynthesis (Teng et al., 2005; Solfanelli et al., 2006). *CINV* (Lou et al., 2007; Barratt et al., 2009) gene expression was enhanced

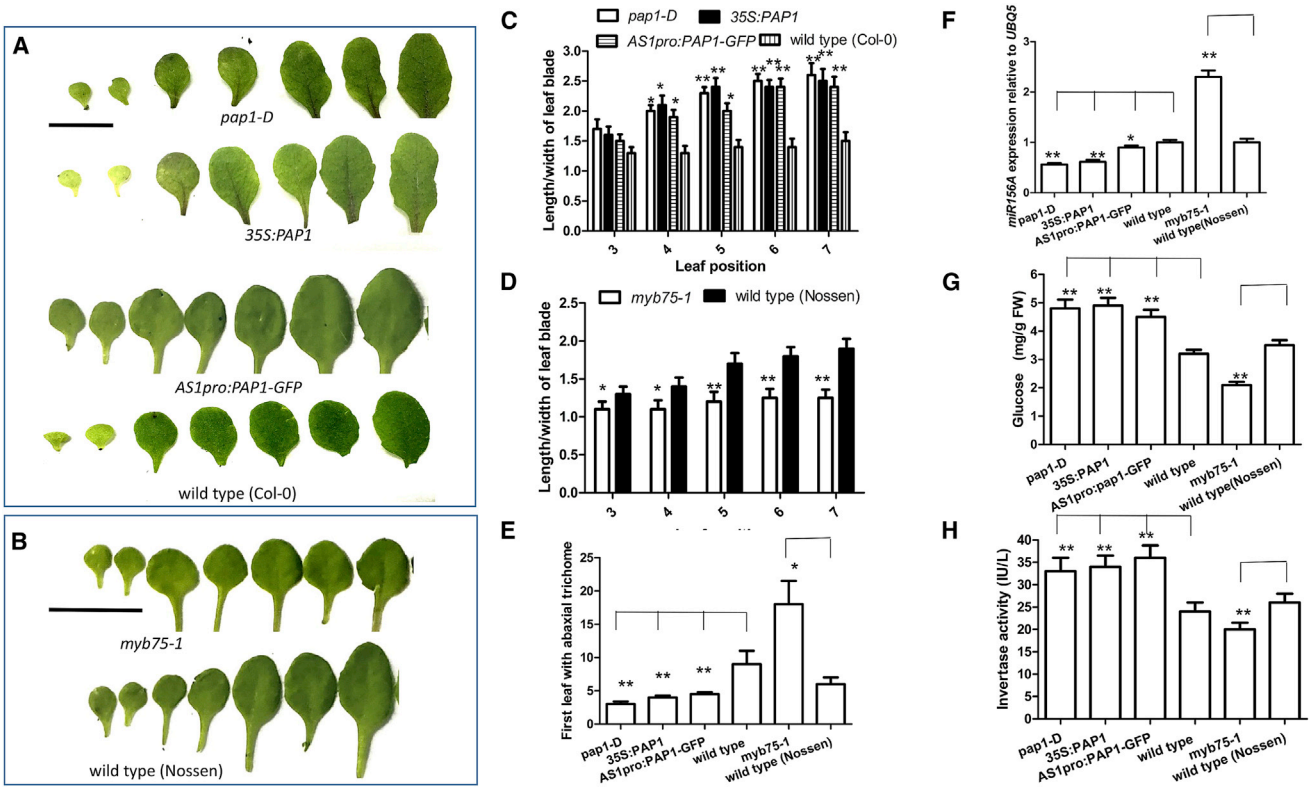

Figure 1. PAP1 promotes the juvenile-to-adult phase transition in *Arabidopsis*

(A) Eighteen-day-old juvenile seedlings of *pap1-D*, *35S:PAP1*, *AS1proPAP1-GFP*, and wild-type (Col-0) plants grown in soil under short days and standard light. Scale bar, 1.0 cm.

(B) Twenty-six-day-old juvenile seedlings of *myb75-1* and wild-type (Nossen) grown in soil under super short days and low light. Scale bar, 1.0 cm.

(C) Bar graph illustrating the length-to-width ratio of leaf blades shown in (A).

(D) Bar graph illustrating the length-to-width ratio of leaf blades shown in (B).

(E) Bar graph illustrating the first leaf with abaxial trichomes as shown in (A) and (B).

(F) Bar graph illustrating *miR156A* expression within the indicated seedlings in (A) and (B). Quantification of wild-type seedlings was set as 1.0 in qPCR analysis. Quantification was normalized to the expression of *UBQ5*.

(G) Bar graph illustrating the glucose levels in the five or six mature leaf blades of the indicated seedlings in (A) and (B).

(H) Bar graph illustrating neutral invertase activity in the five or six mature leaf blades of the indicated seedlings in (A) and (B).

Error bars represent SD (n = 14 in C; n = 18 in D; n = 28 in E; n = 3 in F–H). Student's t test (*$p < 0.05$, **$p < 0.01$).

when the PAP1-related potato MYB transcription factor, *Solanum tuberosum* anthocyanin 1 (*St*AN1), was infiltrated into tobacco leaves (Payyavula et al., 2013). We therefore tested INV activity in our *Arabidopsis* lines expressing PAP1. INV activity was enhanced in the *PAP1* overexpressing plants and was diminished in *myb75-1* plants (Figure 1H). We therefore determined whether *CINV1/2* might be induced by PAP1 in *Arabidopsis*.

CINV1/2 expression was enhanced in *pap1-D* and *35S:PAP1*. In contrast, *CINV1/2* expression was reduced in *myb75-1* plants relative to the wild-type (Figure 2A). Furthermore, the expression of both *PAP1* and *CINV1/2* increased with age (Figures 2B and 2C). Additionally, *CINV1* transcripts were less abundant in 13-, 16-, 19-, and 22-day-old *myb75-1* plants relative to the corresponding wild-type line (Figure 2C). These findings suggest that PAP1 may promote *CINV1/2* expression.

Exogenously supplied sucrose specifically promotes the expression of *PAP1* (Teng et al., 2005), and our data suggest that PAP1 may promote *CINV1/2* expression. Thus, the expression of both *PAP1* and *CINV1* may be mediated by sucrose. To explore this, we monitored both *PAP1* and *CINV1* expression over time in response to sucrose. The expression of both *PAP1* and *CINV1* genes in wild-type seedlings was significantly elevated after sucrose application (Figures 2D and 2E). However, *CINV1* expression in *myb75-1* seedlings was not found to be promoted by transiently applied sucrose (Figure 2F). These findings indicate that PAP1 promotes *CINV1/2* expression, and transiently applied sucrose stimulates *CINV1* expression, which is dependent on PAP1 function.

Since PAP1 promotes *CINV1/2* expression and neutral INV activity was enhanced in the *PAP1* overexpressing plants lines (Figure 1H), we determined whether this PAP1-CINV1/2 pathway also results in enhanced CINV1/2 activity. Our findings indicated that neutral INV activity was decreased in *cinv1/2* (deficient in two closely related isoforms of neutral INV) seedlings (Figure 2G).

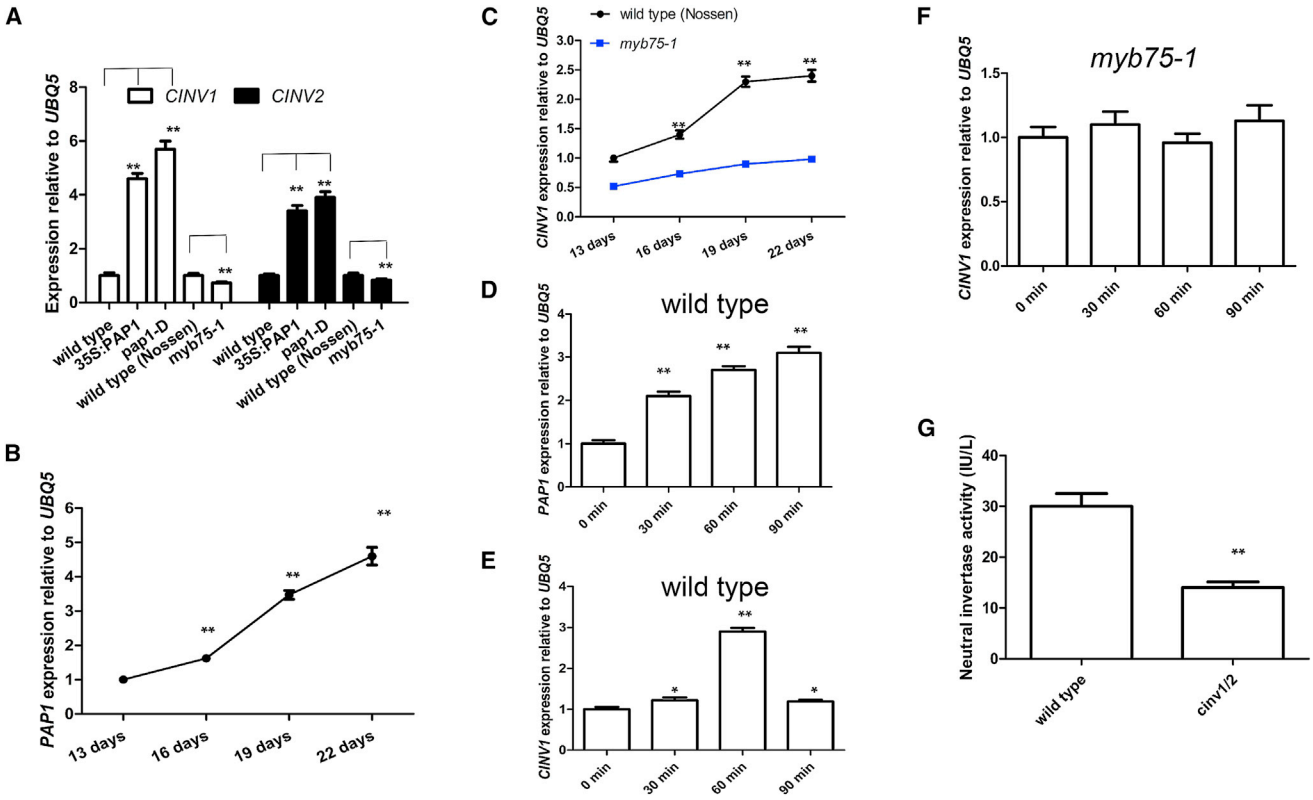

Figure 2. PAP1 positively regulates *CINV1/2* expression

(A) Bar graph showing the differential expression of *CINV1* and *CINV2* among 16-day-old wild-type, *35S:PAP1*, and *pap1-D* grown in soil under short days and standard light or wild-type (Nossen) and *myb75-1* seedlings grown in soil under super short days and low light. The expression of the above genes in wild-type was set as 1.0.

(B) Bar graph showing differential expression of *PAP1* in 13-, 16-, 19-, and 22-day-old wild-type seedlings grown in soil under short days and standard light. Quantification of wild-type seedlings was set as 1.0 in qPCR analysis.

(C) Bar graph showing differential expression of *CINV1* in 13-, 16-, 19-, and 22-day-old wild-type (Nossen) and *myb75-1* seedlings grown in soil under super short days and low light. Quantification of wild-type seedlings was set as 1.0 in qPCR analysis.

(D and E) Bar graph showing differences in the expression levels of *PAP1* (B) and *CINV1* (C) between 6-day-old wild-type seedlings. Wild-type seeds were sown and grown on solid MS medium with 1% sucrose for 6 days, and then seedlings were gathered and treated with double-distilled (dd) water (without sugar as control) and 2% sucrose for 30, 60, and 90 min. Total RNA was extracted from these treated seedlings and qPCR was performed. Quantification of 6-day-old wild-type seedlings treated without sugars was set as 1.0.

(F) Bar graph showing differences in the expression level of *CINV1* between 6-day-old wild-type seedlings. *myb75-1* seeds were sown and grown on solid MS medium with 1% sucrose for 6 days, and then these seedlings were gathered and treated with dd water (without sugars as control) and 2% sucrose for 30, 60, and 90 min. Total RNA was extracted from these treated seedlings and qPCR was performed. Quantification of 6-day-old wild-type seedlings treated without sugars was set as 1.0.

(G) Bar graph illustrating neutral invertase activity in the five or six mature leaf blades in 20-day-old wild-type and *cinv1/2* seedlings.

Error bars represent SD (n = 3). Student's t test (*p < 0.05, **p < 0.01). Quantification was normalized to the expression of *UBQ5*.

Taken together, these findings indicate that PAP1 promotes *CINV1/2* expression and elevates CINV1/2 activity by glucose signaling or by converting sucrose signaling into glucose signaling.

PAP1 directly binds to the *CINV1* promoter, activating its expression

Malus crabapple McMYB10 complements PAP1 function and McMYB10 positively regulates the *Malus* crabapple flavonoid 3′ oxidase (*McF3′H*) via directly interacting with six putative MYB-binding motifs (MYB-BMs): TATCCAACC, AACCTAAC, AAACCA, AACGG, TATCC, and CCAACC (Tian et al., 2015). Thus, to determine whether PAP1 might bind directly to the *CINV1* promoter, we interrogated the promoter sequence of *CINV1* for the presence of MYB-BMs. This search identified seven MYB-BMs and one complementary MYB-BM (GTTAGGTT), designated C1–C8, within the *CINV1* promoter sequence (Figure 3A).

These findings of MYB-BMs within the *CINV1* promoter prompted us to perform chromatin immunoprecipitation (ChIP) analysis. Our data indicated that PAP1 *in vivo* bound to a single MYB-BM (C4, GTTAGGTT) within the *CINV1* promoter sequence but not to other potential MYB-BMs (C1, C2, C3, C5, C6, C7, C8) or the remainder of the promoter sequence of *CINV1* (Figures 3B and 3C). Furthermore, PAP1 binding to the *CINV1* promoter

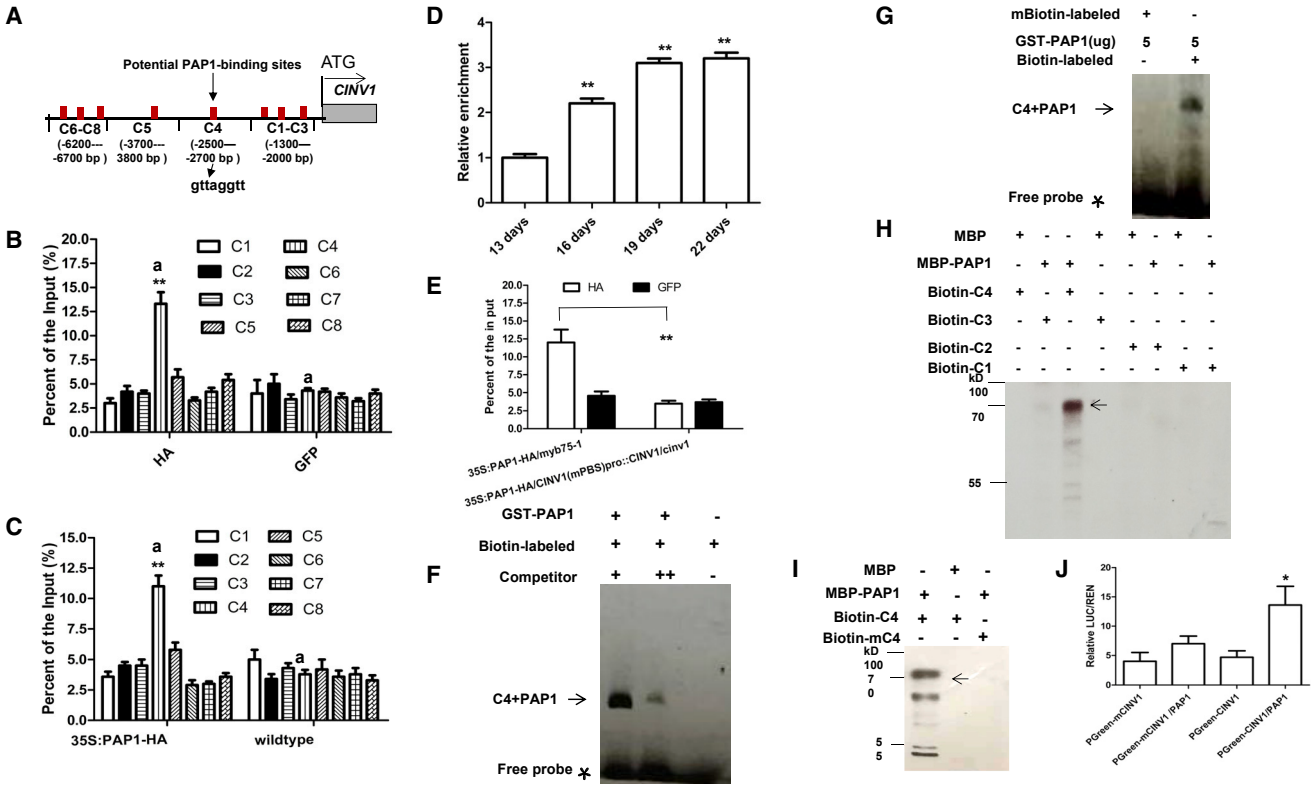

Figure 3. PAP1 directly interacts with the *CINV1* promoter, activating its expression

(A) Schematic of the promoter loci of *CINV1* and its amplicon for ChIP analysis.

(B and C) ChIP-PCR analysis. Enrichment of particular chromatin regions of *CINV1* (B and C) with anti-GFP antibody (as a control in B), wild-type (as a control in C), and anti-HA antibody in *35S:PAP1-HA/myb75-1* seedlings grown on solid MS medium with 1.0% sucrose, as detected by qPCR analysis. Input was set as 100% (supernatant including chromatin [input material] is considered as 100%).

(D) ChIP-PCR over time. Enrichment of particular chromatin regions (C4) of *CINV1* with anti-HA antibody in 13-, 16-, 19-, and 22-day-old *35S:PAP1-HA/myb75-1* seedlings grown in soil under short days and standard light, as detected by qPCR analysis. Thirteen-day-old *35S:PAP1-HA/myb75-1* seedlings was set as 1.0.

(E) ChIP was performed to analyze the *in vivo* interaction between PAP1 and sequence C4 of the *CINV1* promoter. Enrichment is shown of particular chromatin regions of C4 in the *CINV1* promoter with anti-HA antibody or anti-GFP antibody (control) by using 18-day-old-*35S:PAP1-HA/CINV1(mPBS)pro::CINV1-GFP/cinv1* or *35S:PAP1-HA/myb75-1* seedlings, as detected by qPCR analysis.

(F) Unlabeled *CINV1* promoter and unlabeled probes (250 ng [+] and 2.0 mg [++]) were used as competitors to determine the specificity of the DNA-binding activity for PAP1.

(G) A mutant version of the *CINV1* promoter (GGTT/GGAA) was labeled with biotin and used for EMSA with PAP1 polypeptides. Free probe and PAP1 probe complexes are indicated by an asterisk and arrows, respectively, in (F) and (G).

(H and I) Western blot analyses of the indicated proteins pulled down in a protein-DNA pull-down assay with anti-MBP monoclonal antibody. Arrows indicate the degradation fragments of MBP-PAP1.

(J) Bar graph illustrating the relative luciferase luminescence intensities were quantitated using *Renilla* luciferase (REN) for normalization. *CINV1mpro-LUC* indicates the mutated *CINV1pro-LUC* construct.

Error bars represent SD (n = 3). Student's t test (*p < 0.05, **p < 0.01). Quantification was normalized to the expression of *UBQ5* in (B)–(E).

increased over time (Figure 3D), which correlated with an increase of *CINV1* and *PAP1* expression (Figures 2B and 2C). However, a construct, *35S:PAP1-HA/CINV1(mPBS)pro::CINV1-GFP*, which was transformed into the *cinv1* mutant, possessing a mutant binding site for PAP1 (mPBS), exhibited decreased PAP1 binding within the C4 region of the *CINV1* promoter containing the mPBS (Figure 3E).

Moreover, we interrogated the promoter sequence of *CINV2* for the presence of MYB-BMs. This search identified five MYB-BMs in the *CINV2* promoter (Figure S3A). We further performed ChIP analysis to determine whether PAP1 binds to the *CINV2* gene promoter. Our findings indicated that, *in vivo*, PAP1 cannot bind to any MYB-BMs within the *CINV2* promoter sequence (Figure S3B).

Furthermore, electrophoretic mobility shift assay (EMSA) experiments were performed to determine possible *in vitro* direct binding of PAP1 to the C4 sequence within the *CINV1* promoter. PAP1 bound to the labeled C4 sequence *in vitro*, and excessive unlabeled competitor DNA effectively abolished this binding in a dose-dependent manner (Figure 3F). Furthermore, PAP1 did not bind to the corresponding mutated DNA sequence (mC4) (Figure 3G).

To confirm and extend these findings, we performed a DNA-protein pull-down assay. Full-length myelin basic protein

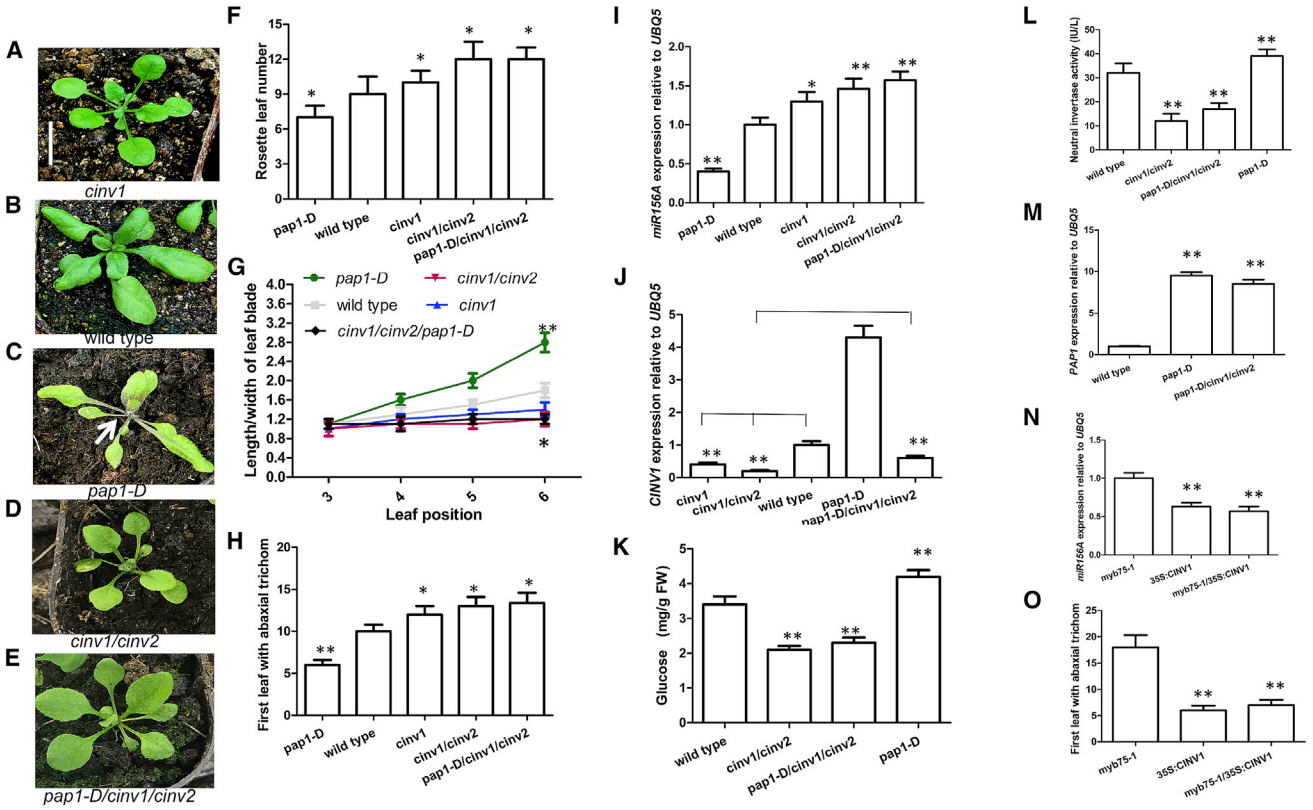

Figure 4. *PAP1* acts upstream of *CINV1* in regulating the juvenile-to-adult phase transition

(A–E) Twenty-day-old seedlings of *cinv1*, wild-type, *pap1-D,* and *pap1-D/cinv1/cinv2* were grown in soil under short days and standard light. Scale bar, 0.5 cm for (A)–(E). White arrows indicate anthocyanin accumulation.

(F) The number of rosette leaves from (A)–(E) in short days.

(G) The length-to-width ratio of the leaf blade from (A)–(E) in short days.

(H) Bar graph illustrating the first leaf with abaxial trichomes in (A)–(E).

(I) Bar graph illustrating *miR156A* expression of the indicated seedlings in (A)–(E). Quantification of wild-type seedlings was set as 1.0 in qPCR analysis.

(J) Bar graph illustrating differences of *CINV1* expression in (A)–(E). The expression of *CINV1* in wild-type seedlings was set as 1.0.

(K) Bar graph illustrating the different glucose concentrations in the five or six mature leaf blades in (A)–(E).

(L) Bar graph illustrating the difference in neutral invertase activity in the five or six mature leaf blades in (A)–(E).

(M) Bar graph illustrating *PAP1* expression in wild-type, *pap1-D*, and *pap1-D/cinv1/cinv2* seedlings. Quantification of wild-type seedlings was set as 1.0 in qPCR analysis.

(N) Bar graph illustrating *miR156A* expression in Figure S5.

(O) Bar graph illustrating the first leaf with abaxial trichomes as shown in Figure S5. Error bars represent SD (n > 12 in F; n > 18 in G; n = 22 in H; n = 16 in O; n = 3 in I–N). Student's t test (*p < 0.05, **p < 0.01). Quantification was normalized to the expression of *UBQ5* in (I), (J), (M), and (N).

(MBP)-PAP1 was pulled down with a *CINV1* promoter fragment C4 but not with C1, C2, or C3 of *CINV1* promoter fragments (Figure 3H), which was consistent with our EMSA data (Figures 3F and 3G). Furthermore, biotin-labeled mutated C4 (mC4) failed to pull down MBP-PAP1 (Figures 3I). Therefore, our findings indicate that PAP1 binds the C4 sequence within the *CINV1* promoter. Finally, transient expression experiments in *Nicotiana benthamiana* showed that co-expression of *PAP1* elevated the expression of a *CINV1pro-LUCIFERASE* (*LUC*) reporter gene (Figure 3J).

Taken together, these data indicate that PAP1 directly binds to the *CINV1* gene promoter to activate *CINV1* expression.

CINV1 promotes the juvenile-to-adult phase transition

Since PAP1 function was associated with the plant juvenile-to-adult phase transition (Figure 1) and PAP1 directly binds to the *CINV1* promoter to transcriptionally activate *CINV1* expression (Figures 2 and 3), we determined whether CINV1 activity may also affect phase transition.

The loss of CINV1 function resulted in small pale green leaves (Lou et al., 2007), consistent with a prolonged juvenile phase relative to wild-type plants. Indeed, compared with the *cinv1* mutant, the *cinv1/cinv2* double mutant showed even smaller pale green leaf blades and a longer juvenile phase (Figures 4A, 4B, and 4D). Thus, the rosette leaf number, the length-to-width ratio in the leaves, the first leaf with abaxial trichomes, and miRNA156A transcripts all showed a prolonged juvenile phase in the *cinv1/cinv2* seedlings (Figures 4F–4I), indicating that CINV1/2 promotes the juvenile-to-adult phase transition. Furthermore, *CINV1* is strongly expressed in mature leaves (Figure S4), suggesting that CINV1 has functions in this organ,

in addition to its role within roots (Lou et al., 2007; Barratt et al., 2009). Therefore, CINV1/2 promotes the juvenile-to-adult phase transition.

Furthermore, we crossed *pap1-D* into the *cinv1/cinv2* double mutant. *PAP1* expression in *pap1-D* and *pap1-D/cinv1/cinv2* plants was not clearly different, excluding the possibility that the transfer DNA (T-DNA) insertions in *cinv1/cinv2* silence the T-DNA insertion in *pap1-D* (Figure 4M). Our findings indicate that the reduced level of both CINV1 and CINV2 activity significantly delayed the juvenile-to-adult transition of *pap1-D* plants (Figures 4A–4I), indicating that CINV1/2 acts downstream of PAP1 to regulate the juvenile-to-adult phase transition. Furthermore, *CINV1* transcript accumulation in leaves of the *pap1-D/cinv1/cinv2* lines was higher than that in *cinv1cinv2* plants (Figure 4J), indicating that PAP1 promotes *CINV1* expression, and these mutants act dependently from each other. Also, endogenous glucose levels were significantly reduced in *cinv1/cinv2* and *pap1-D/cinv1/cinv2* seedlings (Figure 4K), which correlated with a delayed juvenile-to-adult phase transition in these mutants. This may reflect reduced INV activity in *cinv1/cinv2* and *pap1-D/cinv1/cinv2* seedlings (Figure 4L). Taken together, our data show that *CINV1/2* acts downstream of *PAP1* to regulate glucose associated with the juvenile-to-adult phase transition.

To confirm that *CINV1* acts downstream of *PAP1* to promote the juvenile-to-adult transition, we overexpressed *CINV1* or *CINV2* in *myb75-1* plants to determine whether the associated mutant phenotype could be rescued. Our findings indicated that *35S:CINV1* can rescue the *myb75-1* phase transition phenotype (Figures 4N and 4O; Figure S5).

Taken together, our data show that *CINV1* acts downstream of *PAP1* to promote the juvenile-to-adult phase transition.

With increasing age, enhancement of PAP1 transcriptional activity promotes the juvenile-to-adult transition by directly elevating CINV1/2 activity

To monitor the transcriptional activity of PAP1 during the juvenile-to-adult phase transition, we employed a transgenic line containing the *beta-glucuronidase* (*GUS*) reporter gene driven by six tandem repeats of the PAP1 binding site (PBS) (C4) fused to a minimal *35S* promoter (6× *PBS-PAP1::GUS*; Tian et al., 2015). GUS staining intensity over time in the third or fourth leaf of 13-, 16-, 19-, and 22-day-old seedlings gradually increased (Figures S6A and S6B). These findings indicate that PAP1 transcriptional activity is enhanced with age. Furthermore, PAP1 binding to the *CINV1* promoter also increased over time in *35S:PAP1-HA/myb75-1* seedlings (Figure 3D).

GUS staining was observed in the veins of sieve tubes and in companion cells within the phloem (Figure S6C), indicating localized expression of *PAP1* during the juvenile-to-adult phase transition. In sucrose-storing organs, CINV1/2 plays an important function in sugar mobilization (Barnes and Anderson, 2018). Therefore, in a similar fashion to CINV1/2, PAP1 may also have a function related to sucrose mobilization. How this PAP1-CINV1/2 module might regulate sugar mobilization between source and sink requires further exploration.

Collectively, our data indicate that with advancing age, increased PAP1 transcriptional activity promotes the juvenile-to-adult phase transition by directly elevating CINV1/2 activity.

The PAP1-CINV1 module promotes juvenile-to-adult transition by suppression of miR156 in the shoot apex

Our findings show that PAP1 directly and positively regulates the function of CINV1/2 to promote the juvenile-to-adult phase transition (Figures 1–4). miR156 is a central factor in the regulation of the juvenile-to-adult transition, and an increase of sugar promotes *miR156* downregulation to trigger the juvenile-to-adult transition (Yu et al., 2013; Yang et al., 2013). We therefore determined whether the PAP1-CINV1 module was dependent on miR156 function. Thus, we crossed *mir156a-2* into *myb75-1* and *cinv1*. Similarly to *mir156a-2* (Yu et al., 2013), both the length-to-width ratio of leaf blades and the first leaf with abaxial trichomes in the *cinv1/mir156a* and *myb75/mir156a* lines showed a shortened juvenile phase relative to the wild-type (Figures S7A–S7C). Taken together, our data show that the PAP1-CINV1 module promotes the juvenile-to-adult transition by suppression of miR156 in the shoot apex.

SPL9 activates *PAP1* expression

Our data indicate that with increasing age, the PAP1-CINV1/2 module inhibits *miR156-SPL9* expression to promote the juvenile-to-adult transition. We therefore determined whether the transcription factor SPL9 in turn directly regulates *PAP1* expression. We identified putative SPL9 binding sites (GTAC box) within the promoter of *PAP1* (Figure 5A). ChIP analysis indicated that, *in vivo*, SPL9 bound to a P3–P4 promoter sequence of *PAP1* (Figure 5B). Furthermore, EMSA experiments indicated that SPL9 bound to the labeled P3–P4 sequence *in vitro* and that excessive unlabeled competitor DNA effectively abolished this binding (Figure 5C). Furthermore, SPL9 did not bind to the corresponding mutated DNA sequence (mP3–P4) (Figure 5D). Finally, transient expression data in *N. benthamiana* showed that co-expression of *SPL9* increased the expression of a *PAP1pro-LUC* reporter gene (Figures 5E and 5F), indicating that SPL9 directly binds to the *PAP1* gene promoter to activate its expression.

Collectively, our findings show that glucose promotes plant juvenile-to-adult phase transition by the PAP1-CINV1-miR156A/C module (Figures 1, 2, 3, and 4). It has been reported that glucose promotes plant juvenile-to-adult phase transition by the miR156A/C-SPL9 module (Yu et al., 2013; Yang et al., 2013). Furthermore, SPL9 directly activates *PAP1* expression (Figure 5). Therefore, these molecular components may form a glucose feed-forward loop (sucrose-CINV1-glucose-HXK1-miR156A/C-SPL9-PAP1-CINV1-glucose) to control the juvenile-to-adult phase transition.

The glucose feed-forward loop is under dynamic regulation

Our findings indicate that a glucose feed-forward loop controls CINV1/2 activity to convert sucrose into glucose signaling to trigger the juvenile-to-adult transition. Therefore, our glucose feed-forward loop model can predict that with increasing age, an increase of sucrose can induce *PAP1* transcript levels that will lead to transcriptional changes of *CINV1*, *miR156A*, and

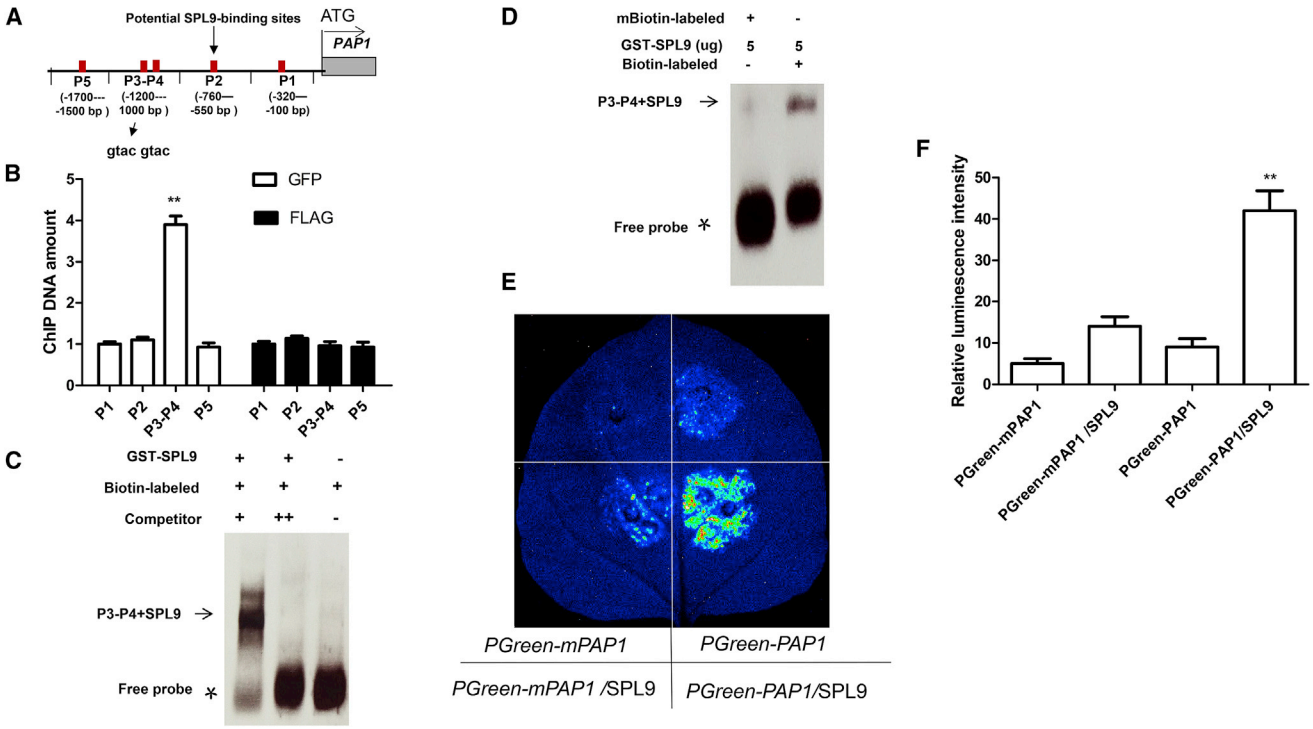

Figure 5. SPL9 directly activates promoter of *PAP1*

(A) Schematic of the promoter loci of *PAP1* and its amplicon for ChIP analysis.

(B) ChIP-PCR analysis. Enrichment of particular chromatin regions of *PAP1* with anti-GFP antibody and anti-FLAG antibody (as a control) in *pSPL9::GFP-rSPL9* seedlings grown in soil, as detected by qPCR analysis. Quantifications were normalized to the expression of *UBQ5*.

(C) Unlabeled *PAP1* promoter and unlabeled probes (250 ng [+] and 2.0 mg [++]) were used as competitors to determine the specificity of the DNA-binding activity for SPL9.

(D) A mutant version of the *PAP1* promoter was labeled with biotin and used for EMSA with SPL9 polypeptides. Free probe and SPL9 probe complexes are indicated by an asterisk and arrows, respectively, in (C) and (D).

(E) Bar graph illustrating transient expression of the 35S:SPL9 effector construct with the *ProPAP1:LUC* reporter construct in *N. benthamiana* leaves. Note *PGreen-mPAP1* indicates that the conserved sites (GTAC) of the region in the *PAP1* promoter were mutated.

(F) Quantitative analysis of luminescence intensity in (E). The luminescence intensity in *PGreen-mPAP1* represents arbitrary luminescence units (~5), and other expression was quantified by using Adobe Photoshop CS (Adobe Systems) software, as described previously by (Meng et al., 2015b).

Error bars represent SD (n = 3 in B; n = 5 in F). Student's t test (**p < 0.01).

SPL9 to trigger the plant juvenile-to-adult transition, due to feed-forward promotion of neutral INV activity. We therefore determined whether this glucose loop is under dynamic regulation.

Sucrose increased over time in wild-type plants (Figure 6A; Yu et al., 2013) and in turn specifically induced *PAP1* transcript accumulation (Figure 2B) and elevated PAP1 levels (Figure 6B). PAP1 in turn activated *CINV1/2* expression by directly binding to its promoter (Figure 3), increasing neutral invertase activity (CINV1/2 activity) (Figure 6C). The resulting glucose signaling inhibited *miR156A* expression and in turn promoted *SPL9* expression (Figures 6D and 6E). Subsequently, SPL9 activated *PAP1* expression by directly binding to its promoter (Figure 5). As a result, *AS1pro:PAP1-GFP* seedlings exhibited an accelerated juvenile-to-adult transition, whereas *cinv1* seedlings were delayed in this process (Figures 6F–6I). Collectively, these findings suggest that this glucose loop is under dynamic regulation.

To confirm and extend these findings, we disrupted a component (PAP1) within this loop. In detail, we generated a transgenic line possessing a *DEXpro:PAP1-GFP* transgene, where the cDNA of *PAP1*, inserted in the antisense orientation, is under the control of a *DEX* (dexamethasone)-inducible promoter. When these *DEXpro:PAP1-GFP* seedlings were grown in soil for 3 days, DEX was applied to inhibit *PAP1* expression. In induced *DEXpro:PAP1-GFP* seedlings, *PAP1* transcript over time is declined relative to the wild-type (Figure S8A), which in turn suppressed *CINV1/2* expression (Figure 3). The resulting neutral INV activity (CINV1/2 activity) decreased (Figure S8B), which may trigger a disruption of glucose signaling. The disrupted glucose signaling promoted *miR156A* expression, which in turn inhibited its target gene, *SPL9* expression (Figures S8C and S8D). Subsequently, SPL9 activated *PAP1* expression by directly binding to its promoter (Figure 5). As a consequence, a reduction of *PAP1* transcripts following induction of *DEXpro:PAP1-GFP* resulted in a delayed juvenile-to-adult transition (Figures S8E–S8G). In aggregate, these data show that the identified glucose feed-forward loop is under dynamic regulation.

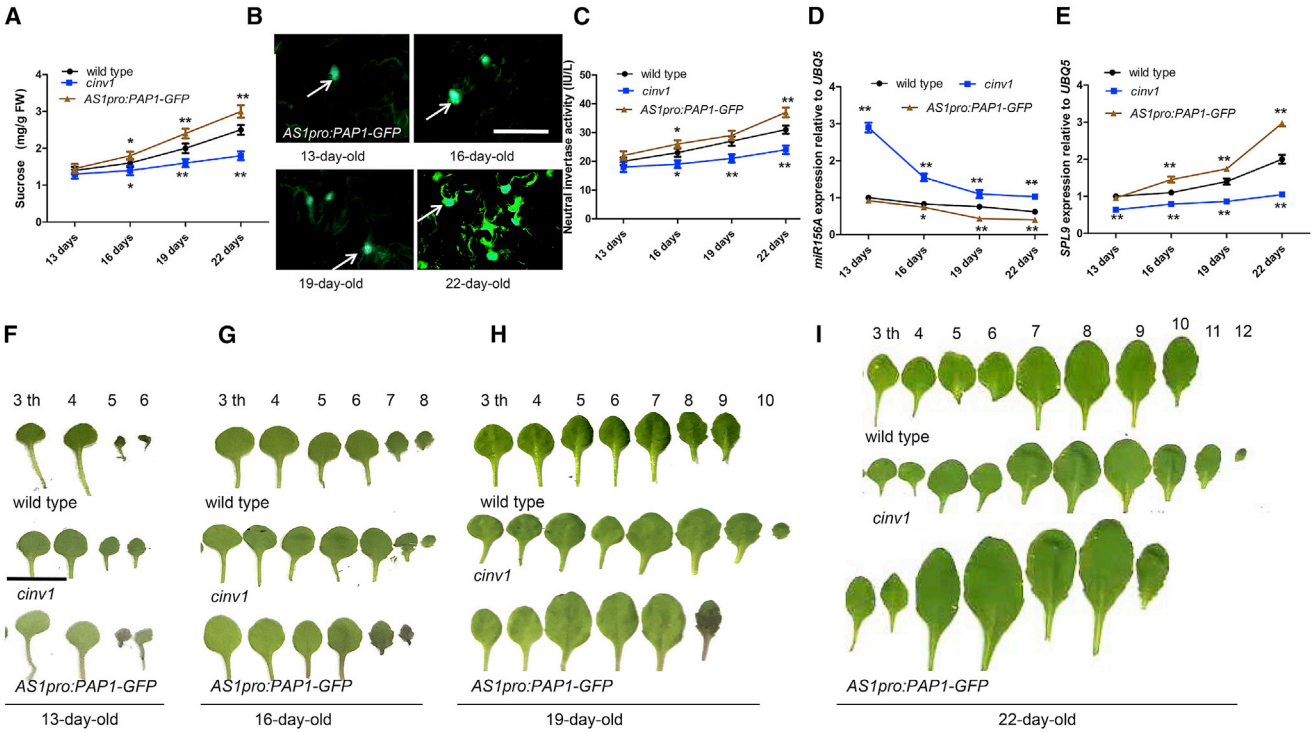

Figure 6. The juvenile-to-adult transition is dynamically regulated by the sucrose-CINV1-glucose-HXK1-miR156-SPL9-PAP1-CINV1-glucose loop

(A) Bar graph illustrating the sucrose levels of leaf blades in 13-, 16-, 19-, and 22-day-old wild-type, *cinv1*, and *AS1proPAP1-GFP* seedlings in (F)–(I). Leaf blades were used for assaying sucrose levels in 13-, 16-, 19-, and 22-day-old seedlings.

(B) Images showing the nuclear localization of AS1pro:PAP1-GFP in leaf blades of 13-, 16-, 19-, and 22-day-old *AS1pro:PAP1-GFP* seedlings. Arrows indicate nuclear localization of PAP1 protein. Scale bar, 500 μm.

(C) Bar graph illustrating neutral invertase activity in leaf blades of the indicated seedlings in (F)–(I). Leaf blades were used for assaying sucrose levels in 13-, 16-, 19-, and 22-day-old seedlings.

(D and E) Bar graph showing the difference in the expression levels of *miR156A* (D) and *SPL9* (E) between 13-, 16-, 19-, and 22-day-old wild-type, *cinv1*, and *AS1proPAP1-GFP* seedlings in (F)–(I). Leaf blades were used for extracting RNA in 13-, 16-, 19-, and 22-day-old seedlings. Quantifications were normalized to *UBQ5* expression. Quantification of wild-type seedlings in (F)–(I) is set as 1.0.

(F–I) The 13-, 16-, 19-, and 22-day-old-seedlings of wild-type, *cinv1*, and *AS1proPAP1-GFP* were grown in soil under short days and standard light. Fully elongated leaf blades were detached and photographed. Error bars represent SD (n = 20). Scale bar, 1.0 cm.

Error bars represent SD (n = 3 in A, B, D, and E). Student 's t test (*$p < 0.05$, **$p < 0.01$).

Sucrose-induced PAP1 directly binds to the *SPL9* promoter to promote a sucrose-mediated juvenile-to-adult transition

Previously, a miR156A/C-SPL9 cascade has been implicated in establishing a sugar-mediated juvenile-to-adult transition (Yang et al., 2013). In this study, we have shown that transcription factor SPL9 activates *PAP1* expression by directly binding to the *PAP1* promoter (Figure 5). In turn, we determined whether the sucrose-induced transcription factor, PAP1, could activate *SPL9* expression by directly binding to the *SPL9* promoter. qPCR analysis indicated that *SPL9* expression was elevated in *pap1-D* and *35S:PAP1* plants and decreased in *myb75-1* plants (Figure 7A). Furthermore, *SPL9* expression was also enhanced in *myb75/mir156a* seedlings (Figure 7A). Collectively, these data suggest that *SPL9* may be a downstream target of PAP1.

We therefore interrogated the promoter sequence of *SPL9* for the presence of MYB-BMs. We identified a number of MYB-BMs in the *SPL9* promoter (Figure 7B). Subsequently, we performed ChIP analysis to determine whether PAP1 directly binds to the *SPL9* promoter. Our findings indicated that, *in vivo*, PAP1 bound to a MYB-BM of *SPL9* (*SPL9* promoter sequence, S2–S3), but not to other MYB-BMs or to the remainder of the promoter sequence of *SPL9* (Figures 7C and 7D). Furthermore, PAP1 association with the *SPL9* promoter increased over time (Figure 7E).

EMSA experiments were performed to determine possible direct *in vitro* binding of PAP1 to the S2–S3 sequence of *SPL9* containing a MYB-BM. Indeed, PAP1 bound to the labeled S2–S3 sequence *in vitro* and excessive unlabeled competitor DNA effectively abolished this binding in a dose-dependent manner (Figure 7F). Furthermore, PAP1 did not bind to the corresponding mutated DNA sequence (mS2–S3) (Figure 7G). Finally, transient expression data in *N. benthamiana* showed that co-expression of *PAP1* increased the expression of a *SPL9pro-LUC* reporter gene (Figure 7H), indicating that PAP1 directly binds to the *SPL9* gene promoter to activate its expression.

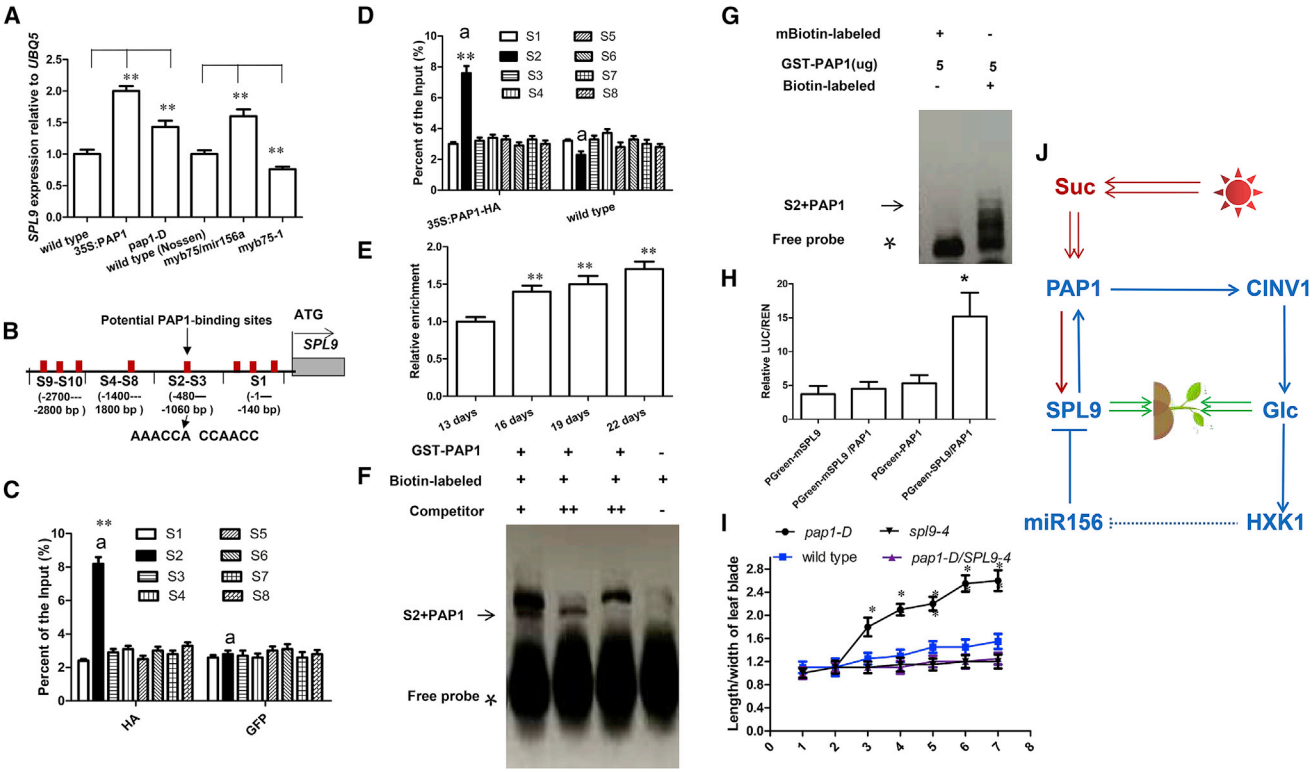

Figure 7. PAP1 directly interacts with the promoter of *SPL9*, activating its expression

(A) Bar graph showing the differential expression of *SPL9* among 14-day-old wild-type, *35S:PAP1*, and *pap1-D* or wild-type (Nossen), *myb75/mir156a*, and *myb75-1* seedlings grown in soil. The expression of these genes in wild-type was set as 1.0.

(B) Schematic of the promoter loci of *SPL9* and its amplicons for ChIP analysis.

(C and D) ChIP analysis. Enrichment of particular chromatin regions of *SPL9* with anti-GFP antibody (as a control in C), wild-type (as a control in D), and anti-HA antibody in *35S:PAP1-HA/myb75-1* seedlings grown in soil, as detected by real-time PCR analysis.

(E) ChIP-PCR over time. Enrichment of particular chromatin regions (S2) of *SPL9* with anti-HA antibody in 13-, 16-, 19-, and 22-day-old *35S:PAP1-HA/myb75-1* seedlings grown in soil under short light conditions, as detected by qPCR analysis. Thirteen-day-old *35S:PAP1-HA/myb75-1* seedlings grown in soil were set as 1.0.

(F) Unlabeled *SPL9* promoter and unlabeled probes (250 ng [+] and 2.0 mg [++]) were used as competitors to determine the specificity of DNA-binding activity for PAP1.

(G) A mutant version of the *CINV1* promoter (AAACCA/TTTCCA or CCAACC/GGAAGG) was labeled with biotin and used for EMSA with PAP1 polypeptides. Free probe and *PAP1* probe complexes are indicated by either an asterisk or arrow, respectively, in (F) and (G).

(H) Bar graph illustrating the relative luciferase luminescence intensities that were quantitated using *Renilla* luciferase (REN) for normalization. *SPL9mpro-LUC* indicates the mutated *SPL9pro-LUC* construct.

(I) Bar graph illustrating the length-to-width ratio of leaf blades in indicated mutant lines grown in soil under short light conditions. Quantification was normalized to the expression of *UBQ5*. Error bars represent SD (n = 3 in A, C, D, and E; n = 5 in H; n = 13 in I). Student's t test (*$p < 0.05$, **$p < 0.01$).

(J) Model illustrating how glucose and sucrose signaling control the juvenile-to-adult transition by the identified glucose feed-forward loop and the sucrose-signaling pathway, respectively. Glucose promotes the juvenile-to-adult phase transition by a glucose feed-forward loop under typical photosynthetic conditions. Sucrose promotes the juvenile-to-adult phase transition by a *PAP1-SPL9* gene cascade under typical photosynthetic conditions. Note that a glucose feedback loop indicates sucrose-CINV1/2-glucose-HXK1-miR156A/C-SPL9-PAP1-CINV1-glucose. Suc, sucrose; Glc, glucose. Arrows and bars represent positive and negative regulation, respectively. Solid lines indicate direct regulation, whereas dotted lines indicate either indirect regulation or regulation in an unknown manner.

spl9-4 single mutant plants presented a delayed juvenile-to-adult phase transition (Figure 7I; phenotype curated by the Arabidopsis Biological Resource Center, The Ohio State University). To determine whether *SPL9* acts downstream of *PAP1* in the regulation of the juvenile-to-adult phase transition, we crossed *pap1-D* into *spl9-4* plants. Our findings indicated that the loss of SPL9 function significantly delayed the juvenile-to-adult transition of *pap1-D* plants (Figure 7I). These findings indicate that *SPL9* acts downstream of *PAP1* to promote the juvenile-to-adult phase transition. Therefore, sucrose-induced PAP1 increases *SPL9* expression and this promotes the sucrose-mediated juvenile-to-adult transition by suppression of miR156 in the shoot apex (Figure 7A).

DISCUSSION

In a similar fashion to animals, plants undergo several key developmental phase transitions in order to reach maturity. It had long been speculated that some of the transitions between these plant developmental stages are triggered by changes in

nutritional status. In both plants and animals, temporally modulated microRNAs (miRNAs) have been identified as master regulators of developmental timing. In *Caenorhabditis elegans*, *LET-7* (Reinhart et al., 2000) and *LIN-4* (Lee et al., 1993), which encode miRNAs, have been identified as key modulators of the juvenile-to-adult transition. In plants, the juvenile-to-adult phase transition is modulated through a temporal decrease in the level of miR156, a central factor in the regulation of this process (Yang et al., 2013).

Previous findings have established that the juvenile-to-adult phase transition was promoted by exogenous sucrose and glucose (Yu et al., 2013; Yang et al., 2013). The loss-of-function chlorophyll-deficient mutant *chlorina1–4* (*ch1–4*) is blocked in the biosynthesis of chlorophyll b and is by extension repressed in carbohydrate production. The *ch1–4* mutant is delayed in the juvenile-to-adult phase transition. Furthermore, this phenotype in *ch1–4* plants can be restored by exogenous glucose. However, the endogenous factors that regulate the juvenile-to-adult phase transition have remained largely unknown.

In this study, we identified CINV1/2 as a key endogenous regulator of phase change. The phenotype of the *cinv1/cinv2* mutant is the best evidence to date that sugar is important for phase change in *Arabidopsis*. It is well established that the gateway of carbon from sucrose into cellular metabolism is controlled principally by CINV1/2 (two of the nine CINV isoforms), but not SUS, because the function of this enzyme is not essential for normal plant growth and development (Barratt et al., 2009).

Our findings reveal that with increasing age, the major photosynthetic product, sucrose, specifically induces *PAP1* expression, which in turn directly elevates CINV1 activity (Figures 3 and 4). The resulting sucrose is irreversibly hydrolyzed by elevated CINV1 activity to produce fructose and glucose. Subsequently, glucose is perceived by the glucose sensor HXK1 (Moore et al., 2003), triggering the juvenile-to-adult phase transition by the miR156A/SPL9 module (Yu et al., 2013; Yang et al., 2013). HXK1 inhibits *miR156* expression by an unidentified regulatory pathway (Yang et al., 2013). SPL9 in turn activates *PAP1* expression (Figure 5). We thus identify a aucrose-CINV1-glucose-HXK1-miR156-SPL9-PAP1-CINV1-glucose loop (Figure 7J). Furthermore, we demonstrated that the glucose feed-forward loop is under dynamic regulation (Figure 6; Figure S8): endogenous glucose accumulation is controlled by CINV1/2 activities regulated by this glucose feed-forward loop to dynamically promote the juvenile-to-adult phase transition (Figure 7J).

In this glucose feed-forward loop, whereas the connections of other components are clear, HXK1 inhibits *miR156* expression by an unidentified regulatory pathway (Yang et al., 2013). HXK1 binds two unconventional partners, the 19S regulatory particle of a proteasome subunit (RPT5B) and the vacuolar H^+-ATPase B1 (VHA-B1). Neither of these proteins has DNA binding capacity, so how this nuclear-localized HXK1 complex regulates gene expression remains unclear. HXK1 interacts with VHA-B1/RPT5B (Cho et al., 2006), with this complex potentially interacting with specific target gene promoters, directly regulating glucose-mediated transcriptional control, for example, at *miR156A/C-SPL9* promoters. Also, an interaction of HXK1 with VHA-B1/RPT5B might be required to increase *miR156A/C* expression. Alternatively, HXK1 might interact with SPL9 and SPL10, which are known to regulate *miR156A/C* expression (Fornara and Coupland, 2009). Exploring these potential mechanisms are an important future research goal.

Biological significance of the glucose feed-forward loop

CINV plays a central role in source-sink regulation (Lou et al., 2007; Barnes and Anderson., 2018). CINV activity is regulated by glucose, as well as by stress-related stimuli and phytohormones (Roitsch, 1999). It has been predicted that any signaling that elevates CINV activities will be maintained and amplified through a positive sugar-signaling loop (Roitsch, 1999; Lou et al., 2007). Thus, in addition to glucose signaling, any other signal network that upregulates CINV activity can in turn promote glucose-signaling-mediated plant growth by this positive sugar-signaling loop. However, it is currently unclear whether any such positive sugar-signaling loops exist.

In this study, we identified a glucose feed-forward loop (sucrose-CINV1-glucose-HXK1-miR156-SPL9-PAP1-CINV1-glucose). CINV1/2 activity, a gateway of carbon entry into cellar metabolism, is a key point of control for the juvenile-to-adult phase transition (Figure 4). In this glucose feed-forward loop, the key components, PAP1 and HXK1, are integration points for multiple cues. The major photosynthetic product, sucrose, specifically induces PAP1 (Teng et al., 2005; Solfanelli et al., 2006), which in turn directly controls CINV1/2 activities (Figures 2 and 3). Furthermore, PAP1 acts as an integration point, receiving diverse internal and external stimuli that modulate plant growth and metabolism (Teng et al., 2005; Das et al., 2012; Jaakola, 2013). Moreover, HXK1 is an additional point of integration for various plant hormones or external stimuli that modulate plant growth and metabolism (Moore et al., 2003). Our findings have therefore provided key insights into the mechanisms of how a vital developmental process in plants is controlled by a gateway for sugars into cellular metabolism (CINV1/2 activity).

A sucrose-signaling pathway regulates the *Arabidopsis* juvenile-to-adult phase transition

Our findings also show that the main photosynthetic product, sucrose, directly and positively regulates the *Arabidopsis* juvenile-to-adult phase transition. Sucrose can specifically induce *PAP1* expression (Teng et al., 2005; Solfanelli et al., 2006), and PAP1 in turn directly binds to the *SPL9* promoter to activate *SPL9* transcription, promoting the *Arabidopsis* juvenile-to-adult transition (Figure 7). Collectively, our findings establish that a sucrose-signaling pathway regulates the *Arabidopsis* juvenile-to-adult phase transition.

Our findings suggest that PAP1 may regulate *SPL9* expression via both a complex cascade (a glucose feed-forward loop) and via direct promoter binding (sucrose-signaling pathway) (Figure 7J). The glucose feed-forward loop can convert sucrose signaling into glucose signaling to promote the *Arabidopsis* juvenile-to-adult phase transition. Therefore, there are two signal inputs on SPL9. PAP1 regulates a glucose feed-forward loop to regulate *SPL9* expression, and PAP1 directly regulates *SPL9* expression by a sucrose-signaling pathway. HXK1 functions in *miR156A/C-SPL9* expression but is not absolutely required for the suppression of *miR156A/C-SPL9* via sugars (Yang et al., 2013; Yu et al., 2013), suggesting that other independent HXK1

regulatory pathways may exist. Indeed, the sucrose-PAP1-SPL9 pathway identified in this study is independent HXK1. Therefore, both sucrose and glucose regulate the juvenile-to-adult transition by distinct pathways, fine-tuning plant growth and development to metabolic status (Figure 7J).

Conclusions

In this work, we identified that PAP1 and CINV1/2 are novel endogenous regulators of the *Arabidopsis* juvenile-to-adult phase transition. Whereas previous work reported that exogenous sugars trigger the juvenile-to-adult phase transition by a miR156A/SPL9 module, the endogenous factors that regulate this process had remained undetermined. Our findings identified CINV1/2 activity as an endogenous factor that regulates the juvenile-to-adult phase transition. More significantly, we identified a glucose feed-forward loop, and this loop is under dynamic regulation to control CINV1/2 activity and shape the juvenile-to-adult phase transition mediated by glucose signaling in *Arabidopsis*. Finally, we identified a sucrose-signaling pathway (PAP1-SPL9 module) that also contributes to the regulation of the *Arabidopsis* juvenile-to-adult phase transition.

STAR★METHODS

Detailed methods are provided in the online version of this paper and include the following:

- KEY RESOURCES TABLE
- RESOURCE AVAILABILITY
  - Lead contact
  - Materials availability
  - Data and code availability
- EXPERIMENTAL MODEL AND SUBJECT DETAILS
- METHOD DETAILS
  - Plant materials and growth conditions
  - Plasmid constructs
  - GUS assay and histochemical analysis of GUS activity
  - ChIP-PCR
  - Quantitative PCR
  - Enzymatic assay of invertase by ELISA
  - Transient assay
  - Test of sugar metabolites
  - Protein expression and purification
  - Electrophoretic mobility shift assay (EMSA)
  - Western blotting and pull-down assay of protein-DNA
- QUANTIFICATION AND STATISTICAL ANALYSIS

SUPPLEMENTAL INFORMATION

Supplemental information can be found online at https://doi.org/10.1016/j.celrep.2021.109348.

ACKNOWLEDGMENTS

This study was supported by the National Science Foundation of China (31401443) and by grants from the Agricultural High Technology Research of Xuzhou City (KC16NG063). *cinv1* (SALK_095807), *pSPL9::GFP-rSPL9*(N9954), *cinv2* (Sail_518_D02), *mir156a-2* (CS71699), and *spl9-4* (Col-0) were obtained from the ABRC (The Ohio State University). The *myb75-1* (pst16228) line was obtained from the RIKEN BioResource Center, which has been characterized genetically and shown to possess a Ds insertion tightly linked to the MYB75 phenotype (Teng et al., 2005). The PAP1-deficient (C24 and Cvi) seeds were kindly provided by Prof. S. Teng (Institute of Plant Physiology and Ecology of Shanghai, Shanghai, China). The *pap-D* mutant (CS3884) was kindly provided by Prof. Su-Sheng Song (Capital University, Nanjing, China). The *pGreen0800-LUC* vector was kindly provided by Prof. Ziqiang Zhu (Nanjing Normal University, Nanjing, China).

AUTHOR CONTRIBUTIONS

L.-S.M. designed experiments. L.-S.M., Q.-X.B., X.-R.M., C.T., C.-Y.L., Y.F., L.-N.X., X.-Y.C., and J.-J.H. performed the experiments. Q.-X.B., X.-R.M., and L.-S.M. completed statistical analysis of data. L.-S.M. and G.J.L. wrote, edited, and revised this manuscript.

DECLARATION OF INTERESTS

The authors declare no competing interests.

Received: December 2, 2020
Revised: April 26, 2021
Accepted: June 15, 2021
Published: July 13, 2021

REFERENCES

Barnes, W.J., and Anderson, C.T. (2018). Cytosolic invertases contribute to cellulose biosynthesis and influence carbon partitioning in seedlings of *Arabidopsis thaliana*. Plant J. *94*, 956–974.

Barratt, D.H.P., Derbyshire, P., Findlay, K., Pike, M., Wellner, N., Lunn, J., Feil, R., Simpson, C., Maule, A.J., and Smith, A.M. (2009). Normal growth of *Arabidopsis* requires cytosolic invertase but not sucrose synthase. Proc. Natl. Acad. Sci. USA *106*, 13124–13129.

Bhargava, A., Mansfield, S.D., Hall, H.C., Douglas, C.J., and Ellis, B.E. (2010). MYB75 functions in regulation of secondary cell wall formation in the Arabidopsis inflorescence stem. Plant Physiol. *154*, 1428–1438.

Cho, Y.H., Yoo, S.D., and Sheen, J. (2006). Regulatory functions of nuclear hexokinase1 complex in glucose signaling. Cell *127*, 579–589.

Das, P.K., Shin, D.H., Choi, S.B., and Park, Y.I. (2012). Sugar-hormone cross-talk in anthocyanin biosynthesis. Mol. Cells *34*, 501–507.

Dharmasiri, N., Dharmasiri, S., and Estelle, M. (2005). The F-box protein TIR1 is an auxin receptor. Nature *435*, 441–445.

Fornara, F., and Coupland, G. (2009). Plant phase transitions make a SPLash. Cell *138*, 625–627.

Gou, J.Y., Felippes, F.F., Liu, C.J., Weigel, D., and Wang, J.W. (2011). Negative regulation of anthocyanin biosynthesis in *Arabidopsis* by a miR156-targeted SPL transcription factor. Plant Cell *23*, 1512–1522.

Guo, M., Thomas, J., Collins, G., and Timmermans, M.C. (2008). Direct repression of *KNOX* loci by the ASYMMETRIC LEAVES1 complex of *Arabidopsis*. Plant Cell *20*, 48–58.

Guo, C., Xu, Y., Shi, M., Lai, Y., Wu, X., Wang, H., Zhu, Z., Poethig, R.S., and Wu, G. (2017). Repression of miR156 by miR159 regulates the timing of the juvenile-to-adult transition in *Arabidopsis*. Plant Cell *29*, 1293–1304.

He, J., Xu, M., Willmann, M.R., McCormick, K., Hu, T., Yang, L., Starker, C.G., Voytas, D.F., Meyers, B.C., and Poethig, R.S. (2018). Threshold-dependent repression of *SPL* gene expression by miR156/miR157 controls vegetative phase change in *Arabidopsis thaliana*. PLoS Genet. *14*, e1007337.

Hsieh, L.C., Lin, S.I., Shih, A.C.C., Chen, J.W., Lin, W.Y., Tseng, C.Y., Li, W.H., and Chiou, T.J. (2009). Uncovering small RNA-mediated responses to phosphate deficiency in *Arabidopsis* by deep sequencing. Plant Physiol. *151*, 2120–2132.

Jaakola, L. (2013). New insights into the regulation of anthocyanin biosynthesis in fruits. Trends Plant Sci. *18*, 477–483.

Jung, J.H., Seo, P.J., Kang, S.K., and Park, C.M. (2011). miR172 signals are incorporated into the miR156 signaling pathway at the *SPL3/4/5* genes in *Arabidopsis* developmental transitions. Plant Mol. Biol. *76*, 35–45.

Jung, J.H., Ju, Y., Seo, P.J., Lee, J.H., and Park, C.M. (2012). The SOC1-SPL module integrates photoperiod and gibberellic acid signals to control flowering time in *Arabidopsis*. Plant J. *69*, 577–588.

Kim, J.J., Lee, J.H., Kim, W., Jung, H.S., Huijser, P., and Ahn, J.H. (2012). The *microRNA156-SQUAMOSA PROMOTER BINDING PROTEIN-LIKE3* module regulates ambient temperature-responsive flowering via *FLOWERING LOCUS T* in *Arabidopsis*. Plant Physiol. *159*, 461–478.

Lee, R.C., Feinbaum, R.L., and Ambros, V. (1993). The C. elegans heterochronic gene *lin-4* encodes small RNAs with antisense complementarity to *lin-14*. Cell *75*, 843–854.

Lee, H., Yoo, S.J., Lee, J.H., Kim, W., Yoo, S.K., Fitzgerald, H., Carrington, J.C., and Ahn, J.H. (2010). Genetic framework for flowering-time regulation by ambient temperature-responsive miRNAs in *Arabidopsis*. Nucleic Acids Res. *38*, 3081–3093.

Li, Z., Peng, J., Wen, X., and Guo, H. (2013). *ETHYLENE-INSENSITIVE3* is a senescence-associated gene that accelerates age-dependent leaf senescence by directly repressing *miR164* transcription in *Arabidopsis*. Plant Cell *25*, 3311–3328.

Lou, Y., Gou, J.Y., and Xue, H.W. (2007). PIP5K9, an *Arabidopsis* phosphatidylinositol monophosphate kinase, interacts with a cytosolic invertase to negatively regulate sugar-mediated root growth. Plant Cell *19*, 163–181.

Mathieu, J., Yant, L.J., Mürdter, F., Küttner, F., and Schmid, M. (2009). Repression of flowering by the miR172 target SMZ. PLoS Biol. *7*, e1000148.

Matsoukas, I.G. (2014). Interplay between sugar and hormone signaling pathways modulate floral signal transduction. Front. Genet. *5*, 218.

Matsoukas, I.G., Massiah, A.J., and Thomas, B. (2013). Starch metabolism and antiflorigenic signals modulate the juvenile-to-adult phase transition in *Arabidopsis*. Plant Cell Environ. *36*, 1802–1811.

May, P., Liao, W., Wu, Y., Shuai, B., McCombie, W.R., Zhang, M.Q., and Liu, Q.A. (2013). The effects of carbon dioxide and temperature on microRNA expression in *Arabidopsis* development. Nat. Commun. *4*, 2145.

Meng, L.S., Wang, Y.B., Yao, S.Q., and Liu, A. (2015a). Arabidopsis AINTEGUMENTA mediates salt tolerance by trans-repressing SCABP8. J. Cell Sci. *128*, 2919–2927.

Meng, L.S., Wang, Z.B., Yao, S.Q., and Liu, A. (2015b). The *ARF2-ANT-COR15A* gene cascade regulates ABA-signaling-mediated resistance of large seeds to drought in *Arabidopsis*. J. Cell Sci. *128*, 3922–3932.

Meng, L.S., Li, Y.Q., Liu, M.Q., and Jiang, J.H. (2016). The *Arabidopsis ANGUSTIFOLIA3-YODA* gene cascade induces anthocyanin accumulation by regulating sucrose levels. Front. Plant Sci. *7*, 1728.

Meng, L.S., Li, C., Xu, M.K., Sun, X.D., Wan, W., Cao, X.Y., Zhang, J.L., and Chen, K.M. (2018a). *Arabidopsis* ANGUSTIFOLIA3 (AN3) is associated with the promoter of *CONSTITUTIVE PHOTOMORPHOGENIC1* (*COP1*) to regulate light-mediated stomatal development. Plant Cell Environ. *41*, 1645–1656.

Meng, L.S., Xu, M.K., Wan, W., Yu, F., Li, C., Wang, J.Y., Wei, Z.Q., Lv, M.J., Cao, X.Y., Li, Z.Y., and Jiang, J.H. (2018b). Sucrose signaling regulates anthocyanin biosynthesis through a MAPK cascade in *Arabidopsis thaliana*. Genetics *210*, 607–619.

Meng, L.S., Wei, Z.Q., Cao, X.Y., Tong, C., Lv, M.J., Yu, F., and Loake, G.J. (2020). Cytosolic invertase-mediated root growth is feedback regulated by a glucose-dependent signaling loop. Plant Physiol. *184*, 895–908.

Moore, B., Zhou, L., Rolland, F., Hall, Q., Cheng, W.H., Liu, Y.X., Hwang, I., Jones, T., and Sheen, J. (2003). Role of the *Arabidopsis* glucose sensor HXK1 in nutrient, light, and hormonal signaling. Science *300*, 332–336.

Payyavula, R.S., Singh, R.K., and Navarre, D.A. (2013). Transcription factors, sucrose, and sucrose metabolic genes interact to regulate potato phenylpropanoid metabolism. J. Exp. Bot. *64*, 5115–5131.

Qi, T., Song, S., Ren, Q., Wu, D., Huang, H., Chen, Y., Fan, M., Peng, W., Ren, C., and Xie, D. (2011). The jasmonate-ZIM-domain proteins interact with the WD-Repeat/bHLH/MYB complexes to regulate jasmonate-mediated anthocyanin accumulation and trichome initiation in *Arabidopsis thaliana*. Plant Cell *23*, 1795–1814.

Reinhart, B.J., Slack, F.J., Basson, M., Pasquinelli, A.E., Bettinger, J.C., Rougvie, A.E., Horvitz, H.R., and Ruvkun, G. (2000). The 21-nucleotide *let-7* RNA regulates developmental timing in *Caenorhabditis elegans*. Nature *403*, 901–906.

Roitsch, T. (1999). Source-sink regulation by sugar and stress. Curr. Opin. Plant Biol. *2*, 198–206.

Rolland, F., Winderickx, J., and Thevelein, J.M. (2001). Glucose-sensing mechanisms in eukaryotic cells. Trends Biochem. Sci. *26*, 310–317.

Schwab, R., Palatnik, J.F., Riester, M., Schommer, C., Schmid, M., and Weigel, D. (2005). Specific effects of microRNAs on the plant transcriptome. Dev. Cell *8*, 517–527.

Schwarz, S., Grande, A.V., Bujdoso, N., Saedler, H., and Huijser, P. (2008). The microRNA regulated SBP-box genes *SPL9* and *SPL15* control shoot maturation in *Arabidopsis*. Plant Mol. Biol. *67*, 183–195.

Sergeeva, L.I., Keurentjes, J.J.B., Bentsink, L., Vonk, J., van der Plas, L.H.W., Koornneef, M., and Vreugdenhil, D. (2006). Vacuolar invertase regulates elongation of *Arabidopsis thaliana* roots as revealed by QTL and mutant analysis. Proc. Natl. Acad. Sci. USA *103*, 2994–2999.

Sgamma, T., Jackson, A., Muleo, R., Thomas, B., and Massiah, A. (2014). *TEMPRANILLO* is a regulator of juvenility in plants. Sci. Rep. *4*, 3704.

Solfanelli, C., Poggi, A., Loreti, E., Alpi, A., and Perata, P. (2006). Sucrose-specific induction of the anthocyanin biosynthetic pathway in *Arabidopsis*. Plant Physiol. *140*, 637–646.

Teng, S., Keurentjes, J., Bentsink, L., Koornneef, M., and Smeekens, S. (2005). Sucrose-specific induction of anthocyanin biosynthesis in Arabidopsis requires the MYB75/PAP1 gene. Plant Physiol. *139*, 1840–1852.

Tian, J., Peng, Z., Zhang, J., Song, T., Wan, H., Zhang, M., and Yao, Y. (2015). McMYB10 regulates coloration via activating *McF3′H* and later structural genes in ever-red leaf crabapple. Plant Biotechnol. J. *13*, 948–961.

Usami, T., Horiguchi, G., Yano, S., and Tsukaya, H. (2009). The more and smaller cells mutants of *Arabidopsis thaliana* identify novel roles for *SQUAMOSA PROMOTER BINDING PROTEIN-LIKE* genes in the control of heteroblasty. Development *136*, 955–964.

Wang, J.W., Czech, B., and Weigel, D. (2009). miR156-regulated SPL transcription factors define an endogenous flowering pathway in *Arabidopsis thaliana*. Cell *138*, 738–749.

Wu, G., Park, M.Y., Conway, S.R., Wang, J.W., Weigel, D., and Poethig, R.S. (2009). The sequential action of miR156 and miR172 regulates developmental timing in *Arabidopsis*. Cell *138*, 750–759.

Xin, M., Wang, Y., Yao, Y., Xie, C., Peng, H., Ni, Z., and Sun, Q. (2010). Diverse set of microRNAs are responsive to powdery mildew infection and heat stress in wheat (*Triticum aestivum* L.). BMC Plant Biol. *10*, 123.

Yamaguchi, A., Wu, M.F., Yang, L., Wu, G., Poethig, R.S., and Wagner, D. (2009). The microRNA-regulated SBP-Box transcription factor SPL3 is a direct upstream activator of *LEAFY*, *FRUITFULL*, and *APETALA1*. Dev. Cell *17*, 268–278.

Yang, L., Xu, M., Koo, Y., He, J., and Poethig, R.S. (2013). Sugar promotes vegetative phase change in *Arabidopsis thaliana* by repressing the expression of *MIR156A* and *MIR156C*. eLife *2*, e00260.

Yu, X., Wang, H., Lu, Y., de Ruiter, M., Cariaso, M., Prins, M., van Tunen, A., and He, Y. (2012). Identification of conserved and novel microRNAs that are responsive to heat stress in *Brassica rapa*. J. Exp. Bot. *63*, 1025–1038.

Yu, S., Cao, L., Zhou, C.M., Zhang, T.Q., Lian, H., Sun, Y., Wu, J., Huang, J., Wang, G., and Wang, J.W. (2013). Sugar is an endogenous cue for juvenile-to-adult phase transition in plants. eLife *2*, e00269.

STAR★METHODS

KEY RESOURCES TABLE

REAGENT or RESOURCE	SOURCE	IDENTIFIER
Critical commercial assays		
GUS staining Kit	COOLABER SCIENCE & TECHNOLOGY Co.,LTD	Cat#SL7160
TRIZOL reagent	Invitrogen, Carlsbad, CA, USA	
the glucose assay kit	Beijing Solarbio Science & Technology Co.,Ltd	Cat#BC2505
Plant Sucrose or Glucose Assay Kit	Beijing Solarbio Science & Technology Co., Ltd, http://www.solarbio.com/goods-9298.html	Cat#BC2465
LightShift Chemiluminescent EMSA Kit	Beyotime Biotechnology	Cat#GS009
Recombinant DNA		
AS1pro::PAP1-GFP	This study	N/A
pGreen-PAP1-LUC	This study	N/A
pGreen-CINV1-LUC	This study	N/A
pGreen-SPL9-LUC	This study	N/A
CINV1mPBSpro::CINV1-GFP	This study	N/A
Oligonucleotides		
Primers used in this study	This study; Table S1	N/A
Experimental models: Organisms/strains		
E. coli (Rosetta2)	N/A	N/A
Agrobacterium tumefaciens (strain GV3101)	N/A	N/A
*Arabidopsis:*WT Col-0	N/A	N/A
Arabidopsis:pap-D mutant (CS3884)	Qi et al., 2011	N/A
Arabidopsis:myb75-1 (pst16228)	Bhargava et al., 2010	N/A
Arabidopsis:mir156a-2 (CS71699)	Yu et al., 2013; Yang et al., 2013	N/A
Arabidopsis:spl9-4 (Col-0)	Wu et al., 2009	N/A
Arabidopsis:CINV1pro-GUS	Meng et al., 2020	N/A
Arabidopsis:cinv2 (Sail_518_D02)	Barratt et al., 2009	N/A
Arabidopsis:cinv1/cinv2	Barratt et al., 2009	N/A
Arabidopsis:pap1-D/spl9	This study	N/A
Arabidopsis:myb75/mir156a	Bhargava et al., 2010	N/A
Arabidopsis:cinv1/mir156a	Bhargava et al., 2010	N/A
Arabidopsis: pap1-D/cinv1/cinv2	Solfanelli et al., 2006; Barratt et al., 2009	N/A
myb75/35S:CINV1	Bhargava et al., 2010; Barratt et al., 2009	N/A
ImageJ	ImageJ	https://imagej.nih.gov/ij/
Graph Pad Prism	Graph Pad Software	https://www.graphpad.com/

RESOURCE AVAILABILITY

Lead contact

Further information and requests for resources and reagents should be directed to and will be fulfilled by the Lead Contact, Lai-Sheng Meng (menglsh@jsnu.edu.cn).

Materials availability

All unique/stable reagents generated in this study are available from the Lead Contact without restriction.

Data and code availability

This paper analyzes existing, publicly available data. These accession numbers for the datasets are listed in the key resources table. This paper does not report original code. "Any additional information required to reanalyze the data reported in this paper is available from the lead contact upon request."

EXPERIMENTAL MODEL AND SUBJECT DETAILS

All plants are in the Col-0 background, unless indicated differently. Plants were grown at short days (10h light/14h dark), super short days (8h light/14h dark), standard light condition (130 μmol quanta PAR m^{-2} s^{-1}) and low light (80 μmol quanta PAR m^{-2} s^{-1}) at 22°C

METHOD DETAILS

Plant materials and growth conditions

pap-D mutant (CS3884) (Qi et al., 2011), *myb75-1* (pst16228) (Bhargava et al., 2010), *mir156a-2* (CS71699) (Yu et al., 2013; Yang et al., 2013), *spl9-4* (Col-0) (Wu et al., 2009), *CINV1pro-GUS* (Meng et al., 2020), *cinv2* (Sail_518_D02) (Barratt et al., 2009) were described previously.

In this work, transgenic plants were generated using the *Agrobacterium tumefaciens* (with used plasmids)-mediated floral dip method (Meng et al., 2015a, 2015b). Transformants were selected on hygromycin B/Kan for three generations followed by analysis of segregation ratios. The plasmids used in this work were introduced into tobacco by *Agrobacterium* mediated-transformation (Meng et al., 2015a, 2015b).

The *cinv1/cinv2* mutant was created by crossing *cinv1* (SALK_095807) with *cinv2* (Sail_518_D02). The absence of *CINV1* and *CINV2* transcripts was confirmed by qPCR (Figures S9A and S9B), as has been described by Barratt et al. (2009). The *pap1-D/spl9* mutant was created via crossing *pap1-D* with *spl9-4.* The absence of *SPL9* transcripts and the overexpression of *PAP1* transcripts were confirmed by qPCR (Figures S9C and S9D). The mutants of *myb75/mir156a* and *cinv1/mir156a* were created by crossing *mir156a-2* with *myb75-1* and *cinv1.* The absences of *mIR156A*, *PAP1* and *CINV1* transcripts were confirmed by qPCR (Figures S9E–S9H). Further, there are pale orange seeds in the siliques of mature plants (Bhargava et al., 2010). We generated an F2 population segregating this mutation, and show that the late trichome phenotype segregates in a 1:3 ratio, and that all of the plants with a late trichome phenotype are homozygous for the *myb75-1* mutation. Used primers were shown in Table S1. The *pap1-D/cinv1/cinv2* mutant was obtained from F2 seedlings of *pap1-D* × *cinv1/cinv2* that purple seeds in the siliques of mature plants (Solfanelli et al., 2006) and had severely shortened roots in 10-day-old seedlings under normal conditions (Barratt et al., 2009). The *myb75/35S:CINV1* mutant was obtained from F2 seedlings of *myb75-1* x *35S:CINV1* that pale orange seeds in the siliques of mature plants (Bhargava et al., 2010) and had elongated roots under normal conditions (Barratt et al., 2009).

Plant growth has been described previously (Meng et al., 2015a, 2015b, 2016) with minor revisions. Short days (10h light/14h dark), super short days (8h light/14h dark), standard light condition (130 μmol quanta PAR m^{-2} s^{-1}) and low light (80 μmol quanta PAR m^{-2} s^{-1}) at 22°C (Yang et al., 2013; Guo et al., 2017). Plants were grown in solid MS medium with sugar concentrations shown in figure legends.

Wild-type is Col-0, unless indicated differently. In all experiments, three biological replicates were performed with similar results and error bars represent SD.

Plasmid constructs

By using gateway methods, as has been described by (Meng et al., 2015a, 2015b, 2016), we obtained the below plasmids. In details, to obtain *DEXpro:PAP1-GFP* and *AS1pro::PAP1-GFP* plasmids, a *PAP1/MYB75* (AT1G56650) CDS and an *AS1* (AT2G37630) promoter were obtained by using specific primers. To obtain *35S:PAP1-HA* and *35S:CINV1* plasmids, a *PAP1/MYB75* (AT1G56650) CDS and a *CINV1* (AT1G35580) CDS were obtained by using specific primers. To obtain *CINV1mPBSpro::CINV1-GFP* plasmids, a *CINV1* (AT1G35580) CDS and promoter were obtained by using specific primers. Please see Table S1 for details on all these primers.

GUS assay and histochemical analysis of GUS activity

The GUS assays were described previously (Meng et al., 2015a, 2015b, 2016). In details, by using a mix buffer [0.1% (v/v) Triton X-100, 0.4 mM of K3Fe(CN)6/K4Fe(CN)6, 60 mM NaPO4 buffer, and 1 mM X-gluc], samples in this work were stained,and then incubated at 37°C for 6-10 h. After GUS staining, chlorophyll was removed using 30, 50, 70, 90 and 100% ethanol about 30 min for every process.

Histochemical analysis of GUS activity was as described (Li et al., 2013). In details, assayed tissues were transferred to microfuge tubes containing a solution of pH 7.0, 10 mM EDTA, 100 mM Na phosphate buffer, 2 mM potassium ferricyanide, 0.1% Triton X-100, 1 mg/mL 5-bromo-4-chloro-3-indolyl-b- D -glucuronide and 2mM potassium ferrocyanide at 37°C overnight. Stained tissues were cleared by using 30, 50, 70, 90 and 100% ethanol about 30 min for every process.

ChIP-PCR

Transgenic lines containing *35S:PAP1:HA/myb75-1* were used in this experiment. ChIP was performed using 15 day-old seedlings grown in short days (Meng et al., 2015a, 2015b, 2016, 2018a, 2018b). Please see Table S1 for details of specific primers.

Quantitative PCR

Total RNA was extracted from tissues indicated in the figures by the TRIZOL reagent (Invitrogen). SYBR green was used to monitor the kinetics of PCR product in real-time RT-PCR. Briefly, first-strand cDNA samples were produced from total RNA samples via reverse transcription using an AMV reverse transcriptase first-strand cDNA synthesis kit (Life Sciences, Promega) and were used as templates for RT- PCR–based gene expression analysis. The expression of *CINV1*, *CNIV2*, *SPL9*, *PAP1* and *miR156A/C* were analyzed by qPCR in wild-type, indicated mutants or overexpressing lines. These primers are listed in Table S1.

Enzymatic assay of invertase by ELISA

Acidic and neutral Invertase in *Arabidopsis* was extracted and purified according to Lou et al. (2007). ELISA was used to assay acidic and invertase activity, as has been described (Meng et al., 2015a, 2015b, 2016, 2018b). In details, the plant N invertase activity assay Kit (Sangon, Shanghai, China) was used in this work. Based on the manufacturer's protocols, in normal sample, and testing medium (48-well plates) with N invertase-antigen, and assayed sample (antibody) were supplemented and incubated in 37°C for 30 min. And then the mixtures were washed for five times to use cleaning solution, and HRP (invertase label) was applied and incubated at 37°C for 30 min for generating antibody−HRP−antigen complexes. When reaction was performed, the mixtures were washed five times utilizing cleaning solution, and then TMB-B and TMB-A were supplemented and incubated at 37°C for 10 min for dyeing. The TMBs were catalyzed through HRP, and then become blue. With termination buffer used, these mixtures became yellow. By using enzyme mark instrument, OD values (450 nm) were assayed. At last, the invertase activity in assayed samples was measured compared with a normal sample.

Transient assay

To produce *CINV1-LUC* and *SPL9-LUC*, the target promoter was amplified via PCR, then inserted into the cloning site of the *pGreen0800-LUC* vector (Meng et al., 2020). See Table S1 for primer. In details. to examine PAP1 activates *CINV1* expression by LUC activity assay, we performed the below experiments. To generate *proCINV1-LUC*, the promoter was PCR amplified with primers *proCINV1-F* and *proCINV1-R* for the gnomic DNA of *Arabidopsis* and inserted into the cloning site of the *pGreen0800-LUC* vector. Used primers can be seen in Table S1. The *MproCINV1-LUC* construct containing mutations in the C4 sequence of the *CINV1* promoter was generated using overlap extension PCR with primers and inserted into *pGreen0800-LUC* vector. Two fragments of *MproCINV1* were combined into a integrated fragments of *MproCINV1* by using primers. To examine PAP1 activates *SPL9* expression by LUC activity assay, we performed the similar experiments.

Used primers can be seen in Table S1.

Test of sugar metabolites

Plant Sucrose or Glucose Assay Kit (Beijing Solarbio Science & Technology Co., Ltd, Cat#BC2465; http://www.solarbio.com/goods-9298.html) was used for assays of sugar metabolites. 0.1g mature leaf blades were ground into homogenate at 23°C, with 0.5 mL extraction buffer and transferred into a centrifuge tube after grinding and kept at 80°C for 10 min, with occasional shaking. After cooling these extracts were centrifuged at 4,000 g for 10 min, the supernatant was transferred to a fresh tube and 2 mg reagent 5 added to decolorize at 80°C for 30 min. Subsequently, 0.5 mL extraction buffer was added, mixed and centrifuged at 4,000 g for 10 min. The supernatant was transferred to a fresh tube for visible light analysis.

Three centrifugal tubes per sample were used with 25 μL of sample. Standard product (reagent 1) and water were added, respectively. Fifteen μL of reagent 2 was added, mixed and boiled at 100°C for 5 minutes. Subsequently, 175 μL of reagent 3 and 50 μL of reagent 4 were added, respectively, followed by boiling in water for 10 min. Light absorption at 480 nm after cooling was undertaken.

Protein expression and purification

In this experiment, the coding sequence in *PAP1* and *SPL9* was amplified, and it was then cloned into *pGEX-5X-1*. Recombinant GST-tagged PAP1 and SPL9 was extracted from transformed *E. coli* (Rosetta2) after 10 h of incubation at 16°C following induction with 10 μM isopropyl β-D-1-thiogalactopyranoside. These recombinant proteins were purified using GST–agarose affinity. Relevant primers are in Table S1.

Electrophoretic mobility shift assay (EMSA)

EMSA was performed as has been described (Meng et al., 2015a, 2015b). Electrophoretic Mobility Shift Assay (EMSA):

The biotin-labeled *CINV1* DNA fragments (5′- gcctatcttgtttgga**gttaggtt**ctaggcaaagcaatggattcgttctct-3′; 5′-agagaacgaatccattg ctttgcctag**aacctaac**tccaaacaagataggc-3′) or mutated *CINV1* DNA fragments (5′-gcctatcttgtttgga**gttaggtt**ctaggcaaagcaatggattcgt tctct-3′;c5′-agagaacgaatccattgctttgcctag**aacctaac**tccaaacaagataggc-3′) were synthesized. The biotin-labeled *SPL9* DNA fragments (5′-catcagttga**aaacca**agtcaaatttatggtagattggcaatggacaaacacaaaatatcatctccatttattg**ccaacc**tcataatg −3′; 5′-cattatga**ggttgg** caataaatggagagatgatatttttgtgtttgtccattgccaatctaccataaatttgact**tggttt**tcaactgatg −3′) or mutated *SPL9* DNA fragments (5′- catcagtt ga**tttcca**agtcaaatttatggtagattggcaatggacaaacacaaaatatcatctccatttattg**ggtacc**tcataatg-3′; c5′-cattatga**aaacca**caataaatggagagatg atattttgtgtttgtccattgccaatctaccataaatttgact**ccaacc**tcaactgatg-3′) were synthesized. They were annealed and used as probes, and the biotin-unlabeled same DNA fragments as competitors in this assay.

The biotin-unlabeled DNA fragments were employed as competitors in the relevant assay. The primer sequences can be found in Supplemental Materials. The probes were incubated with PAP1 at room temperature for 20 mins in a binding buffer (50 mM HEPES-KOH [pH 7.5], 375 mM KCl, 6.25 mM MgCl, 1 mM DTT, 0.5mg/mL BSA, Glycerol 25%). Each 20 mL binding reaction containing 25 fmol Biotin-probe, 6mg protein and 1mg Poly (dIdC) was supplemented to the reaction to minimize nonspecific interactions. The reaction products were analyzed by 6.5% native polyacrylamide gel electrophoresis. Electrophoresis was performed at 120 V for about 1 h in TGE buffer (containing 12.5 mM Tris, 95 mM glycin, 0.5 mM EDTA, pH 8.3, precooled at 210 uC). Gel separated DNA fragments were transferred onto nitrocellulose membrane with 0.5XTBE at 100 V (~400 mA) for 40 mins at 4°C. After cross-linking the transferred DNA to membrane, the membrane was incubated in the blocking buffer for 15 mins with gently shaking, then transferred to conjugate/blocking buffer by mixing 33.3 mL stabilized Streptavidin-Horseradish Peroxidase and conjugate with 10 mL blocking buffer according to manufacturer's protocol (no detail information for the blocking buffer is provided in the kit). The membrane was washed 6 times, each for 5 mins with a washing buffer. Biotin-labeled DNA was detected by the chemiluminescent method according to the manufacture's protocol.

Western blotting and pull-down assay of protein-DNA

The pull-down assay was performed as has been described previously (Dharmasiri et al., 2005) with minor modifications. Probes labeled by 10 pmol biotin were incubated with 10 μL streptavidin magnetic beads for 2 h in the buffer [50 mM KCl, 10 mM Tris·HCl (pH 7.5), 5 mM MgCl 2, 0.05% Nonidet P-40, 3.0% glycerol] and then the free probes were removed by washing out with this buffer. The probe-bound beads were incubated with MBP-PAP1 or 200 ng MBP and then washed five times with 1.0 mL buffer. These precipitates were eluted with SDS loading buffer and analyzed by western-blotting (WB) with anti-MBP monoclonal antibody. 100 μL of buffer supplemented with 10.0 μg BSA and 5 μg fragmented salmon sperm DNA, 100 ng MBP-MBP or MBP were preincubated with 150 pmol of unlabeled probes for 2 h. Subsequently, they were incubated with probe-bound streptavidin magnetic beads (10 μl) labeled by 10 pmol biotin for 2 h. This was followed by five washes with 1.0 mL buffer, these precipitates were eluted using SDS loading buffer and subjected to WB with anti-MBP monoclonal antibody.

QUANTIFICATION AND STATISTICAL ANALYSIS

The length and width of leaf blades were performed using ImageJ. Student's t test was used to determine the statistical significance between wild-type and mutant lines in measure related to glucose and sucrose levels, invertase activity, qPCR, the first leaf with abaxial trichomes, luminescence intensity (*$p < 0.05$; **$p < 0.01$).

Cell Reports, Volume *36*

Supplemental information

Glucose- and sucrose-signaling modules regulate the *Arabidopsis* juvenile-to-adult phase transition

Lai-Sheng Meng, Qin-Xin Bao, Xin-Rong Mu, Chen Tong, Xiao-Ying Cao, Jin-Jin Huang, Li-Na Xue, Chang-Yue Liu, Yue Fei, and Gary J. Loake

Supplemental Information

Glucose and Sucrose Signaling Modules Regulate the *Arabidopsis* Juvenile-to-Adult Phase Transition

Lai-Sheng Meng[1§*], Qin-Xin Bao[1*], Xin-Rong Mu[1*], Chen Tong[1*], Xiao-Ying Cao[1], Jin-Jin Huang[1], Yue Fei[1], Li-Na Xue[1], Chang-Yue Liu[1] and Gary J. Loake[1,2,3§]

Supporting Figures

Supplemental Figure 1. *PAP1* gene expression in selected lines.

Supplemental Figure 2. PAP1 promotes juvenile-to-adult transition in *Arabidopsis*.

Supplemental Figure 3. PAP1 does not directly interact with the promoter of *CINV2*.

Supplemental Figure 4. *CINV1pro-GUS* expression in mature leaves.

Supplemental Figure 5. *PAP1* acts upstream of *CINV1* to positively regulate the *Arabidopsis* juvenile-to-adult transition.

Supplemental Figure 6. Assay of PAP1 function.

Supplemental Figure 7. *PAP1* and *CINV1* act upstream of *miR156A* to positively regulate the *Arabidopsis* juvenile-to-adult phase transition.

Supplemental Figure 8. Juvenile-to-adult transition is dynamically regulated by the Sucrose-CINV1-Glucose-HXK1-miR156-SPL9-PAP1-CINV1-Glucose Loop.

Supplemental Figure 9. Different double mutants were identified by qPCR.

Supporting Tables

Table S1. Used primers in this work.

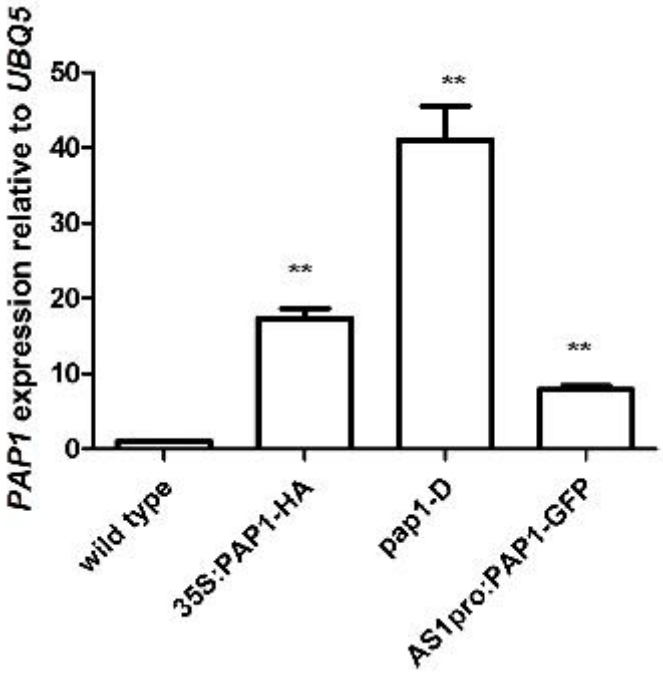

Supplemental Figure 1. *PAP1* gene expression in selected lines, related to Figure 1. Bar graph showing differences in the expression levels of PAP1 between 18 day-old wild-type, *35S:PAP1-HA*, *pap1-D*, and *AS1pro:PAP1-GFP* seedlings grown in soil in short light. Quantifications were normalized to *UBQ5* expression. Quantification of wild-type seedlings is set as 1.0. Error bars represent SD (n=3). Student's *t* test (**P < 0.01).

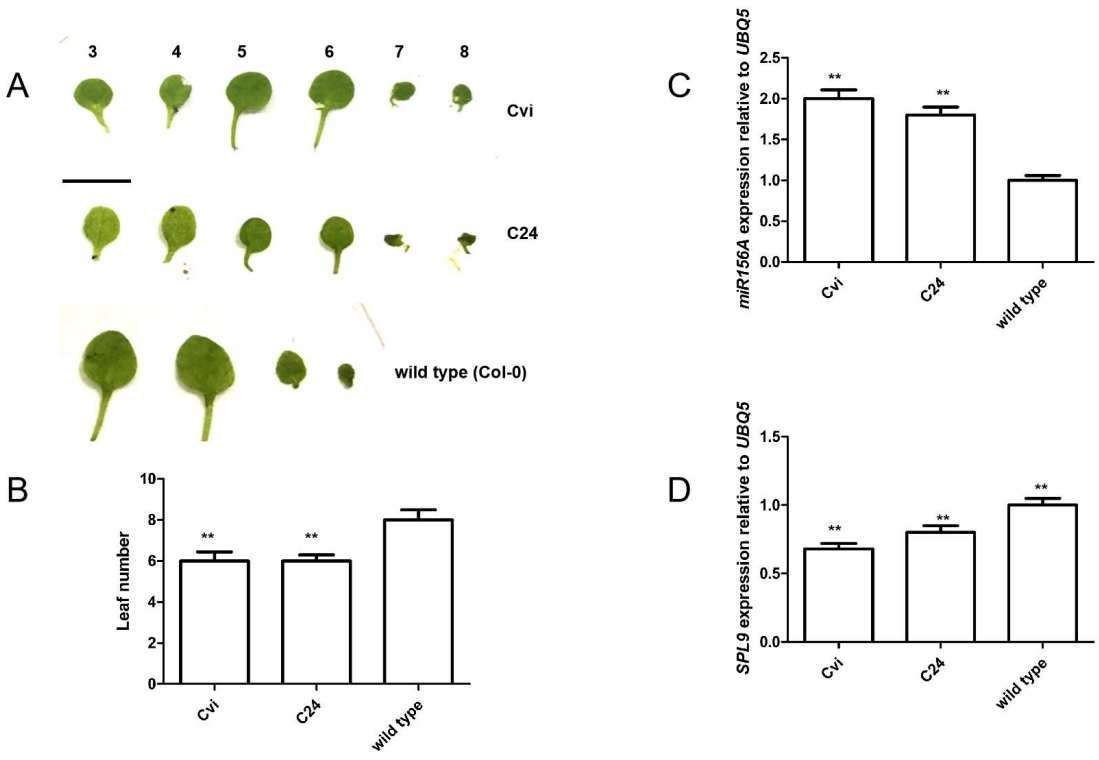

Supplemental Figure 2. PAP1 promotes juvenile-to-adult transition in *Arabidopsis*, related to Figure 1.

A. The 18-day-old-seedlings of wild-type (Col-0), Cvi and C24 grown in soil under short day light (10h light/14h dark, 100 μmol quanta PAR $m^{-2}s^{-1}$ at 22°C). Fully elongated leaf blades were detached and photographed. Bar = 1.0 cm.

B. Bar graph illustrating leaf number in 18-day-old wild-type (Col-0), Cvi and C24 seedlings in A. Error bars represent SD (n=3). Student's *t* test (**P < 0.01; *P < 0.05).

C and D. Bar graph showing the differences in the expression levels of *miR156A* (C) and *SPL9* (D) between 18-day-old wild-type (Col-0), Cvi and C24 in A. Leaf blades were used for extracting RNA at 18-day-old seedlings in short light. Quantifications were normalized to *UBQ5* expression. Quantification of wild-type seedlings in A is set as 1.0. Error bars represent SD (n=3). Student's *t* test (**P < 0.01).

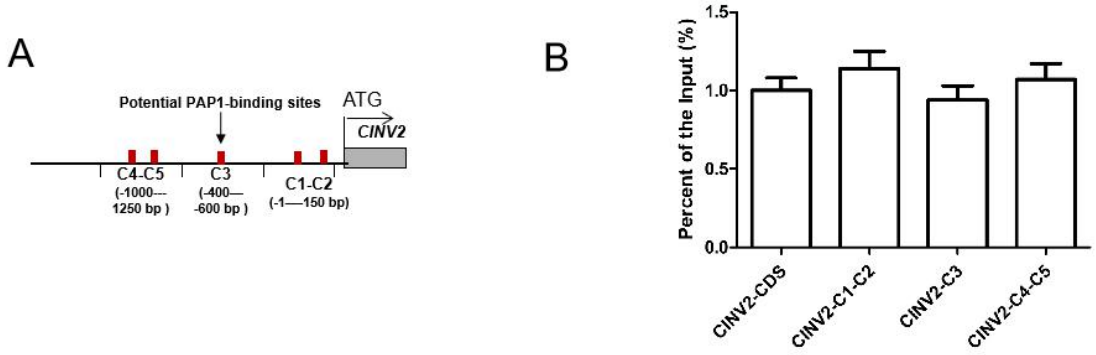

Supplemental Figure 3. PAP1 does not directly interact with the promoter of *CINV2*, related to Figure 3.

A. Schematic of the promoter loci of *CINV2* and its amplicons for ChIP analysis. **B.** ChIP analysis. Enrichment of particular chromatin regions of *CINV2* with anti-HA antibody in 15-day-old *35S:PAP1-HA* transgenic seedlings grown in soil under short days and normal light, as detected by real-time PCR analysis. Quantifications were normalized to the expression of *UBQ5*. Error bars represent SD (n=3). Student's *t* test. Input is set as 100% [supernatant including chromatin (input material) is considered as 100%].

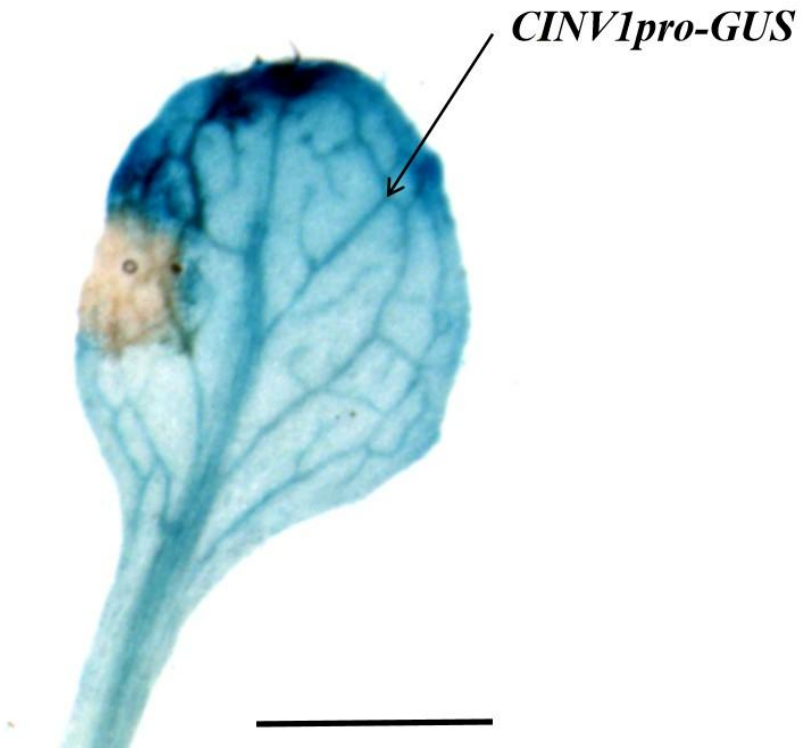

Supplemental Figure 4. *CINV1pro-GUS* expression in mature leaves, related to Figure 4.

Mature leaf blades of 14-day juvenile plants with *CINV1pro-GUS* grown in soil under short days and standard light. Bar = 1.0 cm.

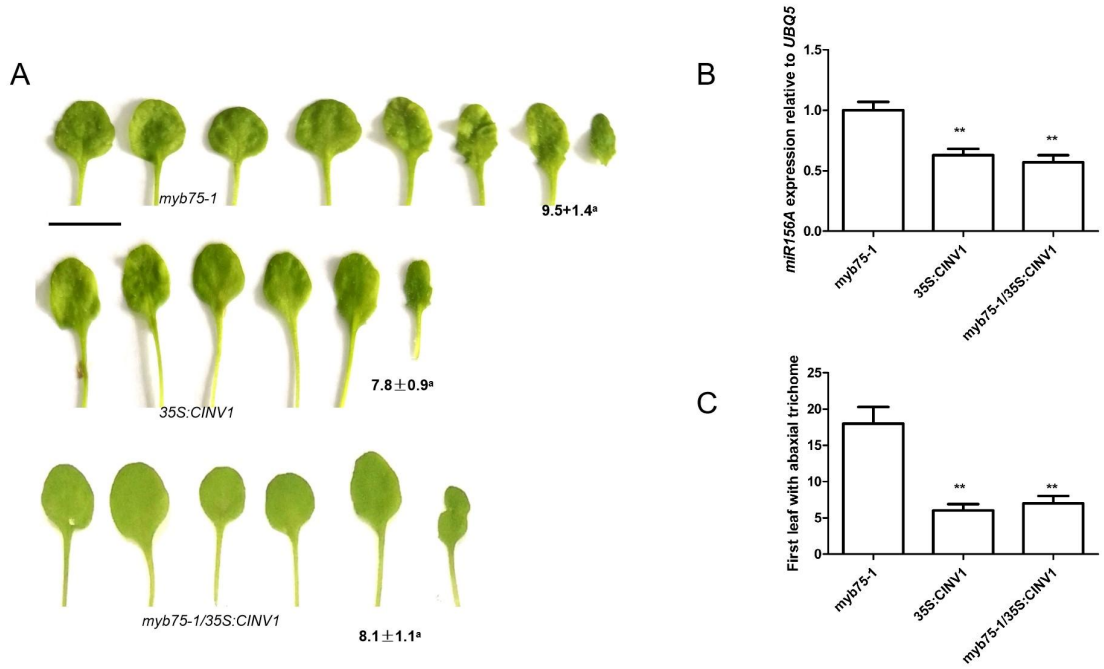

Supplemental Figure 5. PAP1 acts upstream of CINV1 to positively regulate the *Arabidopsis* juvenile-to-adult transition, related to Figure 4.

Twenty-day juvenile plants of *myb75-1*, *35S:CINV1* and *myb75/35S:CINV1* grown in soil under short days and standard light. Fully elongated leaf blades were detached and photographed. Bar = 1.0 cm.

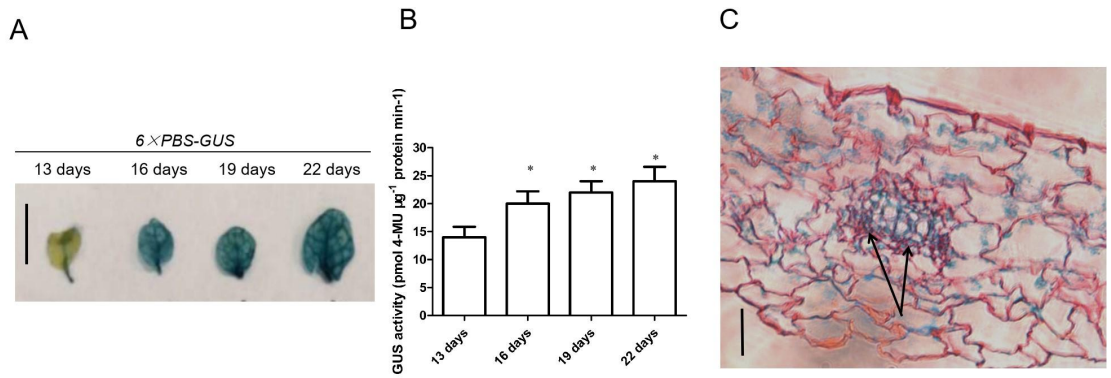

Supplemental Figure 6. Assay of PAP1 function, related to Figure 4.
A, Seedlings of *6×PBS* (*PAP1 binding site*)-*GUS* were grown in soil for 13, 16, 19, 22 days. Subsequently, GUS staining of the 5 or 6th leaf blades from 12 seedlings was performed for 8 hours. Twelve samples had similar results. Bar=2.0 cm. **B**. PAP1 activities (indicated through 6×PBS-GUS activity) of the indicated seedlings in Figure 3K were assayed quantitatively at the indicated time point. GUS activity was measured by picomoles of 4-methyl umbelliferone (4-MU) per mg protein per min. Error bars represent SD (n=3). Student's *t* test (*P < 0.05). **C**. Parafin section of leaf blades. Arrows indicate vascular bundle, and arrows indicate sieve tubes and companion cells in phloem. Bars= 40 μm.

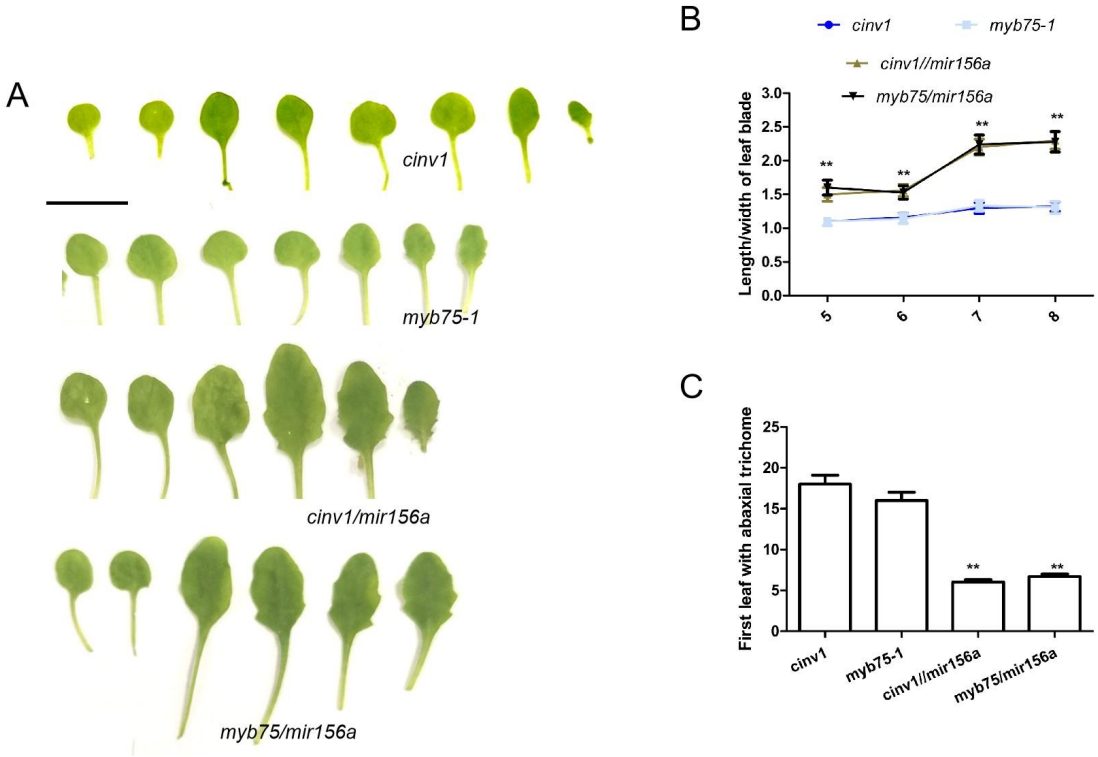

Supplemental Figure 7. *PAP1* and *CINV1* act upstream of *miR156A* to positively regulate the *Arabidopsis* juvenile-to-adult phase transition, related to Figure 4.
(A), Twenty-three-day juvenile plants of *cinv1*, *myb75-1*, *cinv1/mir156a* and *myb75/mir156a* grown in soil under short days and standard light. Fully elongated leaf blades were detached and photographed. Bar = 1.0 cm. (**B**) Bar graph illustrating the ratio of the length-to-width of leaf blades shown in A. (**C**) Bar graph illustrating the first leaf with abaxial trichomes as shown in A.
Error bars represent SD (n=18 in B; n=22 in C). Student's *t* test (**P < 0.01).

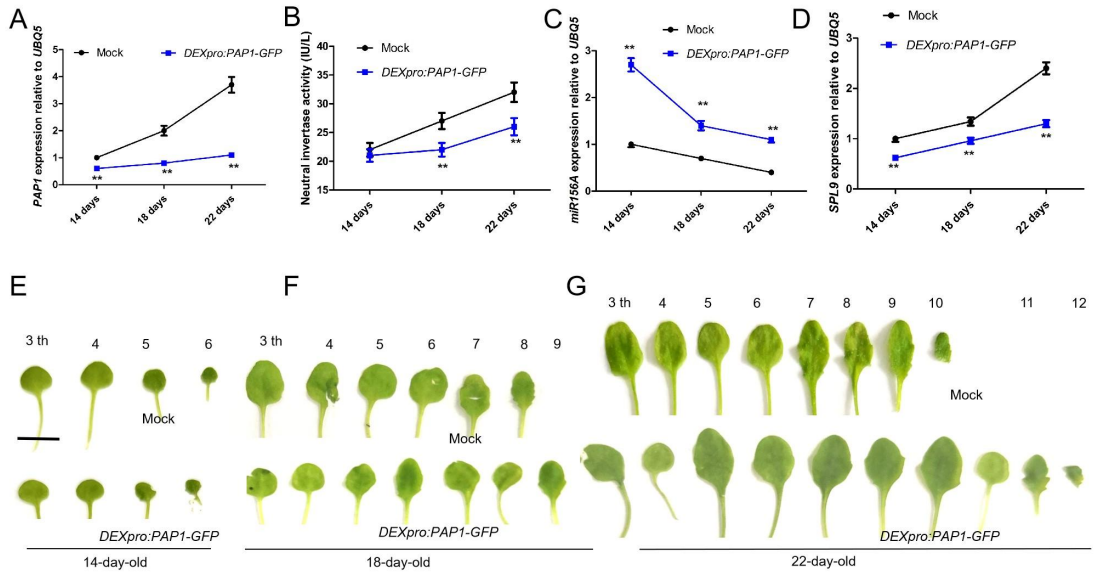

Supplemental Figure 8. Juvenile-to-adult transition is dynamically regulated by the Sucrose-CINV1-Glucose-HXK1-miR156-SPL9-PAP1-CINV1-Glucose Loop, related to Figure 6.

(A) . Bar graph illustrating the *PAP1* expression of leaf blades in 14, 18 and 22-day-old Mock [*DEXpro:PAP1-GFP* (-)] and *DEXpro:PAP1-GFP* (+) seedlings in E-G. *DEXpro:PAP1-GFP* was obtained by that the cDNA of *PAP1* gene was inserted in the antisense orientation and placed downstream of a DEX (dexamethasone)-inducible promoter. Leaf blades were used for assaying sucrose levels at 14, 18, and 22-day-old seedlings. Error bars represent SD (n=3). Student's *t* test (**P < 0.01). Quantifications were normalized to *UBQ5* expression. Quantification of wild-type seedlings is set as 1.0.

(B) . Bar graph illustrating neutral invertase activity in leaf blades of the indicated seedlings in E-G. Error bars represent SD (n=3). Student's *t* test (**P < 0.01). Leaf blades were used for assaying sucrose levels at 14,18, and 22-day-old seedlings.

(C and D). Bar graph showing the difference in the expression levels of *miR156A* (C) and *SPL9* (D) between 14, 18 and 22-day-old Mock [*DEXpro:PAP1-GFP* (-)] and *DEXpro:PAP1-GFP* (+) seedlings in E-G. Leaf blades were used for extracting RNA at 14, 18 and 22-day-old seedlings. Quantifications were normalized to *UBQ5* expression. Quantification of wild-type seedlings in E-G is set as 1.0. Error bars represent SD (n=3). Student's *t* test (**P < 0.01).

(E-G). The 14, 18 and 22-day-old-seedlings of Mock [*DEXpro:PAP1-GFP* (-)] and *DEXpro:PAP1-GFP* (+) were grown in soil under short days and standard light. Fully elongated leaf blades were detached and photographed.

Error bars represent SD (n=16). Student's *t* test (**P < 0.01). Bar = 1.0 cm.

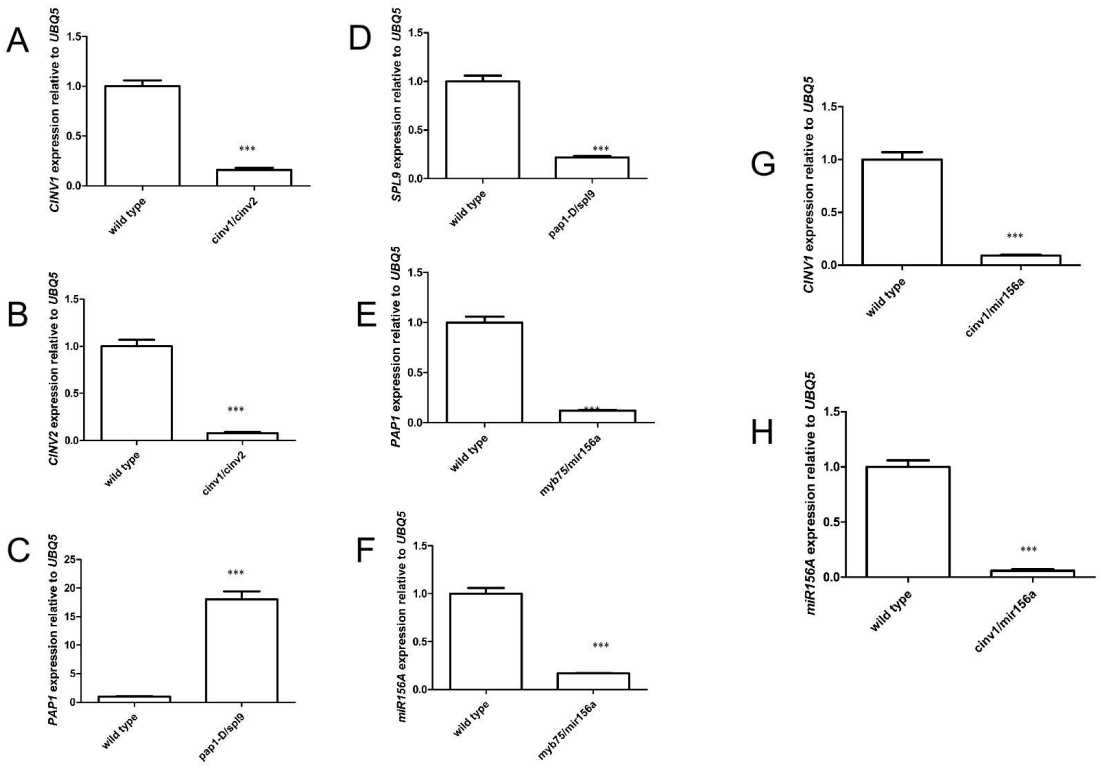

Supplemental Figure 9. Different double mutants were identified by qPCR, related to Star Methods.

(A and **B)** Bar graph showing differential expression of *CINV1* (A) and *CINV2* (B) among 10-day-old wild-type and *cinv1/cinv2* seedlings grown in soil. Quantification was normalized to the expression of *UBQ5.* Quantification of the expression of the above two genes in wild-type seedlings was set as 1.0. Error bars represent SD (n=3). Student's *t* test (***P < 0.001). **(C** and **D)** Bar graph showing differential expression of *PAP1* (C) and *SPL9* (D) among 10-day-old wild-type and *pap1-D/spl9* seedlings grown in soil. Quantification was normalized to the expression of *UBQ5.* Quantification of the expression of the above two genes in wild-type seedlings was set as 1.0. Error bars represent SD (n=3). Student's *t* test (***P < 0.001). **(E** and **F)** Bar graph showing differential expression of *PAP1* (E) and *MIR156A* (F) among 10-day-old wild-type and *myb75/mir156a* seedlings grown in soil. Quantification was normalized to the expression of *UBQ5.* Quantification of the expression of the above two genes in wild-type seedlings was set as 1.0. Error bars represent SD (n=3). Student's *t* test (***P < 0.001). **(G** and **H)** Bar graph showing differential expression of *CINV1* (G) and *MIR156A* (H) among 10-day-old wild-type and *cinv1/mir156a* seedlings grown in soil. Quantification was normalized to the expression of *UBQ5.* Quantification of the expression of the above two genes in wild-type seedlings was set as 1.0. Error bars represent SD (n=3). Student's *t* test (***P < 0.001).

Supplemental Table 1. Primers for Mutant Genotyping, Plasmid Construction, ChIP-PCR, RT-PCR, and Quantitative RT-PCR, related to Star Methods.

Primer Name	DNA Sequence
pCB308R-CINV1-GUS-F	ggg gac aag ttt gta caa aaa agc agg ct aaa ata gaa ata aat caa gaa aag at
pCB308R-CINV1-GUS-R	ggg gac cac tttg tac aag aaa gct ggg t aaa aat ttt gtc gcc aga att t
PAP1-HA-F	ggg gac aag ttt gta caa aaa agc agg ct GAG GGT TCG TCC AAA GGG CT
PAP1-HA-R	ggg gac cac tttg tac aag aaa gct ggg t CTA ATC AAA TTT CAC AGT CTC TC
pMD111-CINV1-GFP plasmid (containing TTCAAA motif)	F- ggg gac aag ttt gta caa aaa agc agg ct aat cga tat taa tta gaa ctc a R- ggg gac cac tttg tac aag aaa gct ggg t ttt tta att att ttg gta ttg ttt ata g
ChIP-PCR-CINV1-C1	F1-ttt gat tct cta ttt gag ata gct R1-ttt tta att att ttg gta ttg ttt ata g
ChIP-PCR-CINV1-C2	F2—cgt aaa tat tga att cca cgt ttc c R2-ttc aag aac atg aaa ttc gta ag
ChIP-PCR-CINV1-C3	F3- ggt ctg ccg gct ttt ata ttt ga R3-aaa aat ttt gtc gcc aga att t
ChIP-PCR-CINV1-C4	F4- ctt tga tgg tat ttc gtt gct g R4-acc tac aga caa aaa gct gat g
ChIP-PCR-CINV1-C5	F5-aaa ata gaa ata aat caa gaa aag at R5-tgc gtt cta att aat atc gat tg
ChIP-PCR-CINV1-C6	F6-ttt att tgg gtt aac aaa acc aa R6-aga att cac gaa ata aga tat ag
ChIP-PCR-CINV1-C7	F7-act caa aat caa tag gta ata a R7-tgt gat taa gtt caa tgt tag ag
ChIP-PCR-CINV1-C8	F8-act aat gtt cat gtt gtc gta ta R8-aca taa aag aaa ttg tta atc cat g
ChIP-PCR-SPL9-S1	F1-gggaagccgaaattttctttgc R1-ttggtttcctcttactcagac

ChIP-PCR-SPL9-S2	F2- gaaaaaaagttttgatattggttcg
	R2-atgtttttccttttggtccacc
ChIP-PCR-SPL9-S3	F3- gaaatataatcgatctctcatattt
	R3-gtacgcttacgactatatttttag
ChIP-PCR-SPL9-S4	F4-caaatttcgacgatagagaccata
	R4-aacacaattttaatttacgtggaac
ChIP-PCR-SPL9-S5	F5- cgccacatgacccatcacta
	R5-aaaaaagaaaccaataaaactttattg
ChIP-PCR-SPL9-S5	F5- cgccacatgacccatcacta
	R5-aaaaaagaaaccaataaaactttattg
CINV1-expression in *pap1-D*	F-5'- ATG GAA GGT GTT GGA CTA AGA
	R-5'- AGA GTA CCA ACA GGT TGA CC -3'
CINV2-expression in *pap1-D*	F-5'- ATG GAG GAA GGT CAT AAA GAA C -3'
	R-5'- GAA AGA ACA CCA TTG ACC TTC T -3'
PAP1-expression in *cinv1/2,35S:CINV1*	F-5'- ATG GAG GGT TCG TCC AAA GG -3'
	R-5'- CTT CCA GCA ATT AAA GAC CAC C -3'
PAP1-expression protein	F-5'- ATG GAG GGT TCG TCC AAA GG -3'
	R-5'- CTT CCA GCA ATT AAA GAC CAC C -3'
CINV1-expression in wild type*, cinv1, cinv1/cinv2, pap1-D* and *pap1-D/cinv1/cinv2*	F-5'- ATG GAA GGT GTT GGA CTA AGA
	R-5'- AGA GTA CCA ACA GGT TGA CC -3'
SPL9-expression in *pap1-D, 35S:PAP1*	F-5'- TTG GCC AGA AGA TCT ACT TCG
	R-5'- GTT TGA ACG ACC ACC TGA GGA -3'
The expressions of *SPL9* in the *35S:PAP1-HA* seedlings	F-5'- TTG GCC AGA AGA TCT ACT TCG
	R-5'- GTT TGA ACG ACC ACC TGA GGA -3'
The expressions of *CINV1* in the *35S:PAP1-HA* seedlings	F-5'- ATG GAA GGT GTT GGA CTA AGA
	R-5'- AGA GTA CCA ACA GGT TGA CC -3'
The expressions of *miR156A* in the *35S:PAP1-HA* seedlings	F-5'- CAA GAG AAA CGC AAA GAA ACT G
	R-5'-GAG ATC AGC ACC GGA ATC TG -3'
The expressions of *miR156A* in the 5 and 70 day-old wild type seedlings	F-5'- CAA GAG AAA CGC AAA GAA ACT G
	R-5'-GAG ATC AGC ACC GGA ATC TG -3'

The expressions of *miR156A* in the *35S:PAP1* and *pap1-D* seedlings
F-5'- CAA GAG AAA CGC AAA GAA ACT G
R-5'-GAG ATC AGC ACC GGA ATC TG -3'

The expressions of *miR156C* in the *35S:PAP1* and *pap1-D* seedlings
F-5'- CGC ATA GAA ACT GAC AGA AGA
R-5'- CGG AAT CTG ACA GAT AGA GCA-3'

The expressions of *HXK1* in the *35S:PAP1* and *pap1-D* seedlings
F-5'- TGC GGT GGC TGT TTT GGT TG
R-5'- TTG TCT CAG TTT CGA GAT CGG-3'

To gain *AS1pro::PAP1-GFP*, the below primers were used.
CEII-proAS1-F：CAGCTATGACATGATTACGAATTCtcaaagcaggcccatccaagg
AS1-PAP1-FP-R：CGAACCCTCCATctcctactcctcctgacatcac
AS1-PAP1-FP-F：ggaggagtaggagATGGAGGGTTCGTCCAAAGG
CEII-PAP1-R：CTCGCCCTTGCTCACCATAAGCTTATCAAATTTCACAGTCTCTCCATCG

To gain *pGreen-PAP1-LUC*, the below primers were used.
pGreen-PAP1pF:Ttcctgcagcccgggggatccaatgacttaatctcgtaacgagtcac
pGreen-PAP1pR:Tgtttttggcgtcttccatggggaacaaagatagatacgtaaaatatataa
PAP1pm1R:gctttcttgcatgaaaatttacgtggccgatggaaaacctaggcgaaatgata
PAP1pm2F:Tatcatttcgcctaggttttccatcggccacgtaaattttcatgcaagaaagc
PAP1pm2R: attttctaagaaaagcatttttagtcggccttttgaggacttgcaatttaaa
PAP1pm3F: Tttaaattgcaagtcctcaaaaaggccgactaaaaatgcttttcttagaaaat

To gain *pGreen-CINV1-LUC*, the below primers were used.
pGreen-CINV1pF:Ttcctgcagcccgggggatcctgggagacttgtatcgatggtggtg
pGreen-CINV1pR:Tgtttttggcgtcttccatggataacactaaaccaagatctaaaatc
CINV1pm1R:ttaagaaaccaaagtaggataccat**ttgcca**tataaaagccggcagaccaacaaaa
CINV1pm2F:ttttgttggtctgccggcttttata**tggcaa**atggtatcctactttggtttcttaa

To gain *pGreen-SPL9-LUC*, the below primers were used.
pGreen-SPL9pF:Ttcctgcagcccgggggatcccgccacatgacccatcactatcacgg
pGreen-SPL9pR:Tgtttttggcgtcttccatgggttggtttcctcttactcagacagaa
SPL9pm1R:Tgccaatctaccataaatttgacttggccttcaactgatgaatgcgaaccaatat
SPL9pm2F:atattggttcgcattcatcagttgaaggccaagtcaaatttatggtagattggca
SPL9pm2R:ttggtccaccatttggcattatgagcatcgcaataaatggagatgatattttgtgtttg
SPL9pm3F:caaacacaaaatatcatctccatttattgcgatgctcataatgccaaatggtggaccaa

To gain *CINV1mPBSpro::CINV1-GFP*, the below primers were used.
CEII-proCINV1-F CAGCTATGACATGATTACGAATTCgtgtccccatttttggctgtg
MproCINV1(PBS)-FP-R gctttgcctagtccaaacaagataggctagtaggtagc
MproCINV1(PBS)-FP-F ctagcctatcttgtttggactaggcaaagcaatggattcg
FP-proCINV1-CINV1-R GTCCAACACCTTCCATtataacactaaaccaagatctaaaatcaaaac
FP-proCINV1-CINV1-F agatcttggtttagtgttataATGGAAGGTGTTGGACTAAGAG
CEII-CINV1-R CTCGCCCTTGCTCACCATAAGCTTGAGTTGTGGCCAAGACGCAG